© 2014. Published by The Company of Biologists Ltd | The Journal of Experimental Biology (2014) 217, 758-768 doi:10.1242/jeb.089904

RESEARCH ARTICLE

An experimental and morphometric test of the relationship between vertebral morphology and joint stiffness in Nile crocodiles (*Crocodylus niloticus*)

Julia L. Molnar*, Stephanie E. Pierce and John R. Hutchinson

ABSTRACT

Despite their semi-aquatic mode of life, modern crocodylians use a wide range of terrestrial locomotor behaviours, including asymmetrical gaits otherwise only found in mammals. The key to these diverse abilities may lie in the axial skeleton. Correlations between vertebral morphology and both intervertebral joint stiffness and locomotor behaviour have been found in other animals, but the vertebral mechanics of crocodylians have not yet been experimentally and quantitatively tested. We measured the passive mechanics and morphology of the thoracolumbar vertebral column in *Crocodylus niloticus* in order to validate a method to infer intervertebral joint stiffness based on morphology. Passive stiffness of eight thoracic and lumbar joints was tested in dorsal extension, ventral flexion and mediolateral flexion using cadaveric specimens. Fifteen measurements that we deemed to be potential correlates of stiffness were taken from each vertebra and statistically tested for correlation with joint stiffness. We found that the vertebral column of *C. niloticus* is stiffer in dorsoventral flexion than in lateral flexion and, in contrast to that of many mammals, shows an increase in joint stiffness in the lumbar region. Our findings suggest that the role of the axial column in crocodylian locomotion may be functionally different from that in mammals, even during analogous gaits. A moderate proportion of variation in joint stiffness (R^2=0.279–0.520) was predicted by centrum width and height, neural spine angle and lamina width. These results support the possible utility of some vertebral morphometrics in predicting mechanical properties of the vertebral column in crocodiles, which also should be useful for forming functional hypotheses of axial motion during locomotion in extinct archosaurs.

KEY WORDS: Crocodylomorph, Evolution, Locomotion, Biomechanics, Morphometrics, Spine

INTRODUCTION

Modern crocodylians are secondarily adapted to a semi-aquatic mode of life. However, they use a wide range of terrestrial locomotor behaviours, ranging from a sprawling 'belly crawl' to more erect 'high walking' and asymmetrical gaits such as bounding and galloping that are otherwise found only in mammals (Renous et al., 2002). The terrestrial abilities of modern crocodylians are thought to have been inherited from their Triassic ancestors, which had a more erect posture, possibly great athleticism on land, and more terrestrial lifestyles (Parrish, 1987). While many studies of crocodylian locomotion have sought to unravel the function of the limbs during variable locomotor behaviours (e.g. Blob and Biewener, 1999; Gatesy, 1991; Reilly and Elias, 1998; Reilly et al., 2005; Willey et al., 2004), the importance of the axial skeleton has received far less attention. Yet kinematic studies have revealed an appreciable role for both dorsoventral and mediolateral vertebral movements during terrestrial locomotion in crocodylians (e.g. Carpenter, 2009; Gatesy, 1991; Reilly and Elias, 1998; Renous et al., 2002).

Crocodylian bracing system

The axial morphology of crocodylians and their ancestors has been proposed to be closely tied to the evolution of locomotor performance (Frey, 1988; Frey and Salisbury, 2001; Salisbury and Frey, 2000; Schwarz-Wings et al., 2009). These studies inferred that a 'bracing system' composed of osteodermal armour, vertebrae, ribs and axial musculature keeps vertebral loads low and assists in gravitational support. In contrast to the bracing system of early crocodylomorphs, which 'nearly prevented' mediolateral movements and was specialized for cursoriality, that of modern crocodylians is thought to permit both dorsoventral and mediolateral movements during terrestrial and aquatic locomotion (Frey, 1988). Evolutionary changes in the morphology of the bracing system, specifically the opening of the margins of the paravertebral shield and the loss of articulating processes between the osteoderms, may explain why crocodylomorphs transitioned from one vertebral form (amphicoelous) to another (procoelous) and why body size is tightly linked to locomotor ability in some crocodylians (Salisbury and Frey, 2000; Schwarz-Wings et al., 2009). Additionally, the bracing system has been proposed to be the critical anatomical structure influencing athletic capacity, perhaps even more important than other factors such as limb forces (Salisbury and Frey, 2000). The idea that the crocodylian bracing system functions as intuitively as described has long been accepted without quantitative biomechanical testing. Here, we aimed to perform such an experimental test on one component of the bracing system by measuring the stiffness of crocodylian intervertebral joints, as we explain below.

Intervertebral joint stiffness

Intervertebral joint stiffness is relevant to locomotion because it affects force transmission, passive maintenance of posture, and the speed and amplitude of travelling or fixed waves of undulation (Gál, 1993a; Hebrank et al., 1990; Long, 1992; Long et al., 1997; McHenry et al., 1995). Consider the mechanical behaviour of a relatively stiff vertebral column versus a more flexible one: the stiff column requires greater work (produced by muscles or external forces such as gravity and inertia) to produce bending, which translates into more powerful (and possibly more energetically costly) active movement. For example, the lumbosacral joint in

Structure & Motion Laboratory, Department of Comparative Biomedical Sciences, The Royal Veterinary College, Hawkshead Lane, Hatfield AL9 7TA, UK.

*Author for correspondence (jmolnar@rvc.ac.uk)

Received 20 April 2013; Accepted 29 October 2013

The Journal of Experimental Biology

The Journal of Experimental Biology (2014) doi:10.1242/jeb.089904

many terrestrial mammals is less stiff than the other lumbar intervertebral joints, which may enhance pelvic girdle and hindlimb movement (Gál, 1993a). In passive support, a stiff column can sustain greater gravitational moments with smaller displacements, conserving energy in postural muscles. Examples include passive resistance to 'hogging' moments of the mid-trunk in terrestrial quadrupeds (Christian and Preuschoft, 1996) and ventral flexion moments produced by the weight of the head and upper body in seated macaques (Gál, 2002). In swimming, stiffness in the vertebral column may serve to decelerate the tail in dolphins, and variation in stiffness along the column may produce patterns of deformation during locomotion, i.e. less stiff regions would have greater angular deflections (Long et al., 1997) [but see Nowroozi and Brainerd for a notable exception (Nowroozi and Brainerd, 2013)]. A stiffer column has a higher undulatory frequency and propagates travelling waves more quickly, resulting in a faster swimming speed (Long, 1992). Mechanically relevant properties such as stiffness and range of motion have also been linked to athletic ability and locomotor habits in several fish and mammalian species (e.g. Gál, 1993a; Hebrank et al., 1990; Long, 1992; Long et al., 1997), but they have not been quantitatively studied in crocodylians.

Vertebral morphology and function

Understanding the relationship between bone morphology and functional characteristics, such as intervertebral joint stiffness, is fundamental to our interpretation of fossils, and thus to our understanding of the evolution of locomotion. All such interpretations are complicated by the unknown quantities of soft tissues such as skin and muscle, and they are especially difficult in the vertebral column where mobility is constrained by the intervertebral discs or notochord, fibrous tissues and ligaments (Gál, 1993b; Koob and Long, 2000). Morphometric measurement of vertebrae is a promising approach to this problem, because experimental evidence supports correlation of stiffness with such characteristics as the presence of zygapophyses, intervertebral disc length and width (which can be estimated from centrum dimensions), centrum length, nucleus pulposus length and transverse process height (Hebrank et al., 1990; Long, 1992; Long et al., 1997; Slijper, 1946). The contribution of vertebral processes to joint stiffness has been assessed by testing stiffness before and after their removal, with mixed results; Gaudin and Biewener (Gaudin and Biewener, 1992) found that xenarthrae did not contribute significantly to stiffness in any direction in armadillos, but Hebrank et al. (Hebrank et al., 1990) found that haemal spines and zygapophyses both stiffened intervertebral joints in marlins. However, these laws cannot be indiscriminately applied to crocodylians because stiffness appears to be governed by different structures in different species (Gál, 1993a).

In addition to joint stiffness, vertebral morphology also has been found to correlate with locomotor behaviour and mechanics, including swimming style, habitual spinal loading patterns and arboreal locomotor habits. In pinnipeds, relative centrum length and width, transverse process width and inter-zygapophyseal length were correlated with swimming style (pelvic versus pectoral oscillation) (Pierce et al., 2011), and in whales centrum length and width were correlated with degree of dorsoventral flexion and undulatory wavelength during swimming (Buchholtz, 2001). In a range of mammals, relationships have been found between habitual spinal loading patterns (dorsoventral shear, mediolateral shear, torsion, axial compression) and centrum width, mediolateral spacing of zygapophyses and zygapophyseal angle (Boszczyk et al., 2001), and between arboreal locomotor habits and neural spine height and angle, transverse process width, lamina width and pre-zygapophyseal angle (Shapiro, 2007). The principles drawn from living animals also have been applied to reconstruct locomotor behaviour in extinct relatives (e.g. Buchholtz, 2001; Buchholtz, 2007; Finch and Freedman, 1986; Hua, 2003; Piechowski and Dzik, 2010; Pierce et al., 2011; Pittman et al., 2013; Shapiro et al., 2005).

Study aims

To test the validity of inferring locomotor biomechanics from vertebral morphology, we quantified the passive stiffness of intervertebral joints along the thoracolumbar region in cadaveric Nile crocodiles (*Crocodylus niloticus* Laurenti 1768), and we investigated the relationship between intervertebral joint stiffness and vertebral morphological variation. Although our approach measures passive stiffness of individual joints (here simply termed 'joint stiffness') and not factors such as muscle-driven mechanics, dynamic behaviour of viscoelastic tissues, or other axial structures such as ribs and osteoderms, it does test how some of the components of the bracing system work. By doing so, we sought to begin to answer fundamental questions about how the crocodylian vertebral column functions in a locomotor context. For instance, do the mechanical properties of the crocodylian vertebral column support a role in locomotion (especially asymmetrical gaits) similar to its role in mammals, or are there marked differences? And if so, can the mechanical differences be correlated with anatomical ones? By comparing regional anatomical variation with direct measurements of joint stiffness in *C. niloticus*, we also hope to identify those morphological parameters that have the greatest power to predict vertebral mechanics in extant crocodiles, and, with due caution, in their extinct relatives.

RESULTS

Variation in stiffness

Joint stiffness in all directions increased slightly or remained constant along the thoracic vertebral column and increased significantly at the lumbar and lumbosacral joints (Fig. 1). This

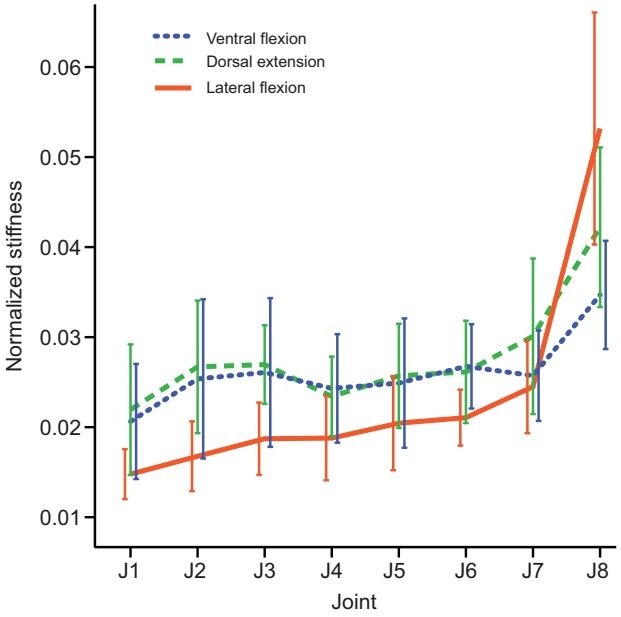

Fig. 1. Average normalized joint stiffness of *Crocodylus niloticus*, from most cranial (J1) through to most caudal (J8) joints for all three bending directions. The graphs show that stiffness is highest in dorsal extension, and stiffness in all bending directions increases with craniocaudal position of the joint. Error bars represent 1 s.d.

The Journal of Experimental Biology (2014) doi:10.1242/jeb.089904

Table 1. Variation in stiffness between joints and bending directions

A. Summary of *F*-values			*F*	*P*
Joint position (7)			19.482	<0.0001
Bending direction (2)			8.311	<0.0001
Bending direction × joint position (14)			1.716	0.0610
B. Summary of significant *post hoc* tests				
Pairwise comparisons		Mean difference	s.e.	*P*
Dorsal extension	Lateral flexion	0.105	0.038	0.0181
Lateral flexion	Ventral flexion	−0.112	0.038	0.0103
J1	J5	−0.235	0.063	0.0068
	J6	−0.274	0.063	0.0006
	J7	−0.394	0.063	0.0000
	J8	−0.844	0.064	0.0000
J2	J7	−0.227	0.062	0.0089
	J8	−0.677	0.063	0.0000
J3	J7	−0.206	0.061	0.0242
	J8	−0.656	0.062	0.0000
J4	J7	−0.236	0.061	0.0040
	J8	−0.686	0.062	0.0000
J5	J8	−0.609	0.062	0.0000
J6	J8	−0.570	0.062	0.0000
J7	J8	−0.450	0.062	0.0000

(A) Summary of *F*-values (type III sums of squares) from ANOVA with normalised stiffness as the dependent variable. Degrees of freedom (d.f.) are given in parentheses to the right of each factor; error d.f. were 122. Sample size was 146.
(B) Bonferroni *post hoc* tests were conducted on significant factors in the ANOVA. Only significant differences after accounting for multiple comparisons are reported. See Fig. 3 for joints. See supplementary material Table S7 for all pairwise comparisons.

effect was particularly pronounced in lateral flexion. Stiffness was lowest in lateral flexion in all joints except the lumbosacral, where it was the highest. Significant differences in stiffness were found with position of the joint along the column ('joint', $P<0.0001$) and bending direction ('direction', $P<0.0001$) (Table 1A). Stiffness was significantly lower in lateral flexion than in dorsal extension ($P=0.0181$) or ventral flexion ($P=0.0103$). J8 was significantly stiffer than all other joints ($P<0.0001$); J6 was significantly stiffer than J1 ($P=0.0006$); J7 was significantly stiffer than each of the four more cranial joints ($0.0001<P<0.0242$); and J5 was significantly stiffer than J1 ($P=0.0068$). *P*-values reflect Bonferroni corrections for multiple comparisons. Severing intervertebral ligaments resulted in a small but significant increase in stiffness ($P=0.002$), although a substantial increase of 1.8±0.1 deg in the neutral zone ($P<0.0001$) may account for this effect.

Variation in morphology

For descriptive purposes, the vertebral column is divided into four regions, cranial thoracic (T1–T4), caudal thoracic (T5–L1), lumbar (L2–L5) and sacral (S1), based upon changes in the values and trends of morphological measurements (Fig. 2). In the cranial thoracic region, there was a sharp gradient between characteristic cervical and thoracic morphologies. The caudal thoracic region showed a more gradual change: centrum length, width and height, transverse process width and pre-zygapophyseal angle increased in a caudad direction, and neural spine height decreased. Transverse process orientation shifted from being caudally and dorsally directed to approach an angle of 180 deg in both planes. Within the lumbar region, transverse processes decreased in width, increased in length and inclined caudally, while the centra became shorter and wider. The first sacral vertebra showed sharp increases in the length and width of the centrum and transverse processes (related to articulation with the iliac bones). Many of the morphological parameters were strongly inter-correlated (see supplementary material Table S1).

Correlates of stiffness

Several morphological parameters were found to be significant correlates of stiffness (Table 2). Pre-zygapophyseal width, inter-zygapophyseal length and ventral deflection of transverse processes were correlated positively with stiffness in all directions ($0.0001<P<0.0443$), and neural spine angle was correlated negatively with stiffness in all directions ($0.0001<P<0.0024$). Centrum height was positively correlated with stiffness in dorsal extension ($P=0.0048$) and ventral flexion ($P=0.0116$), and lamina width was correlated positively with stiffness in dorsal extension ($P=0.0042$) and lateral flexion ($P=0.0093$). Additional parameters were correlated with stiffness in lateral flexion only: pre-zygapophyseal angle ($P=0.0058$), neural spine length ($P=0.0166$) and centrum length ($P=0.0455$) in a positive direction and neural spine height ($P=0.0443$) in a negative direction.

Predictors of stiffness

An initial stepwise linear regression, using all morphometric measurements as potential predictors, resulted in models where dorsal extension was predicted ($R^2=0.470$) by pre-zygapophyseal width ($P<0.001$) and centrum width ($P=0.003$); lateral flexion was predicted ($R^2=0.624$) by pre-zygapophyseal width ($P=0.001$) and transverse process deflection both ventrally ($P<0.0001$) and caudad ($P=0.0002$); and ventral flexion was predicted ($R^2=0.385$) by neural spine angle ($P<0.0001$) and neural spine height ($P=0.006$) (see supplementary material Table S2). Collinearity statistics indicated problems for the lateral flexion and ventral flexion models, with the majority of tolerances below 0.6; to address this problem, we conducted a principal components analysis (PCA) to uncover uncorrelated morphological parameters. The PCA produced a subset of six measurements (lamina width, neural spine angle, caudal deflection of transverse processes, transverse process tip length, centrum width, centrum height) that were minimally correlated with each other (absolute value of Pearson correlation <0.35) (see supplementary material Table S1), yet each measurement was

The Journal of Experimental Biology (2014) doi:10.1242/jeb.089904

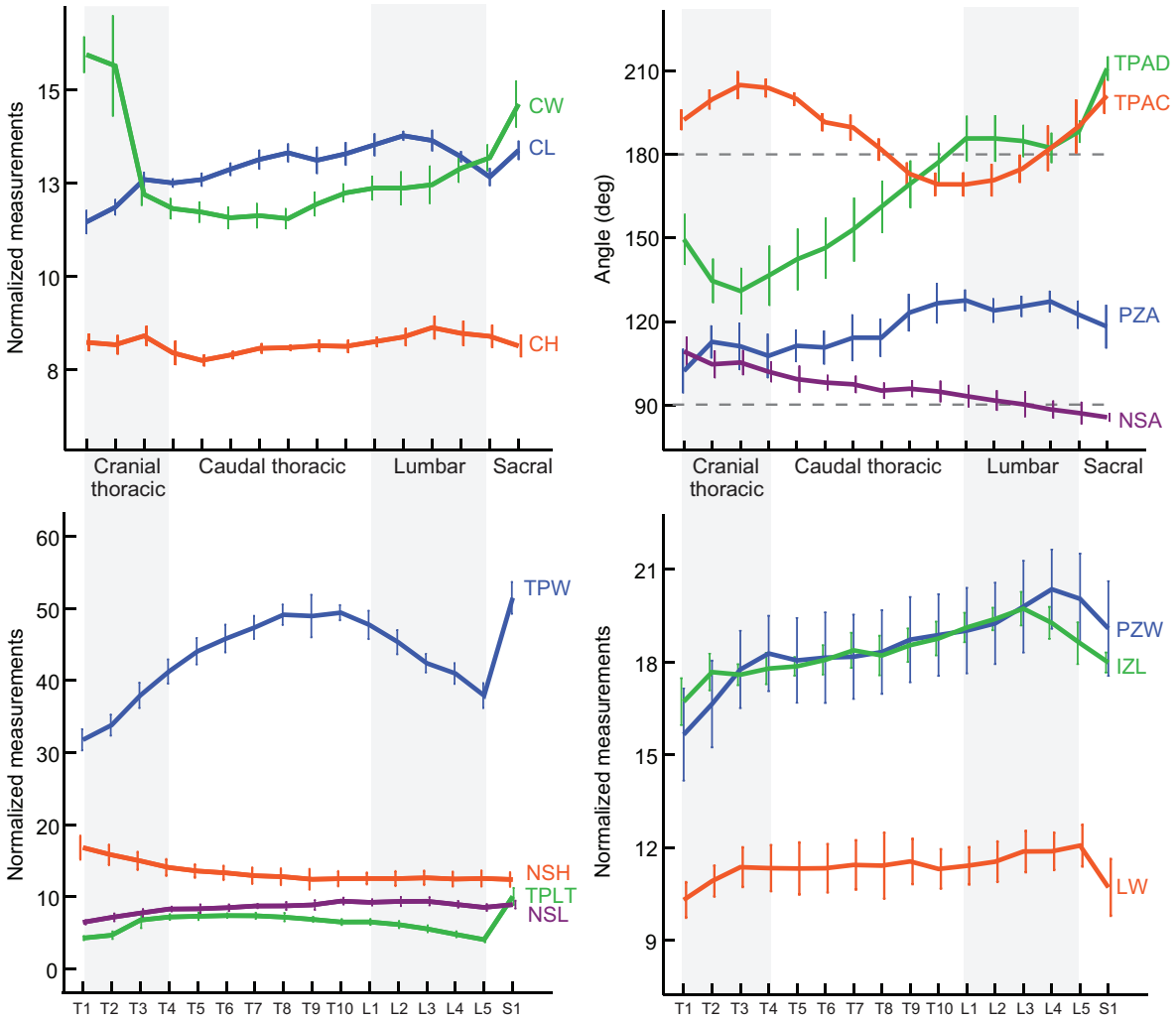

Fig. 2. Variation in morphometric measurements along the vertebral column. Grey shading indicates anatomical regions (cranial thoracic, caudal thoracic, lumbar, sacral) used to describe changes in morphology. Linear measurements were normalized by thoracolumbar length, approximated by the sum of centrum lengths. Transverse process angles greater than 180 deg indicate caudal and ventral deflection, and neural spine angles greater than 90 deg indicate caudal deflection. Pre-zygapophyseal angles greater than 90 deg indicate that facets are oriented closer to horizontal than vertical. Error bars represent 1 s.d. CW, centrum width; CL, centrum length; CH, centrum height; TPAD, dorsoventral transverse process angle; TPAC, craniocaudal transverse process angle; PZA, pre-zygapophyseal angle; NSA, neural spine angle; TPW, transverse process width; NSH, neural spine height; NSL, neural spine length; TPLT, transverse process length at tip; PZW, pre-zygapophyseal width; IZL, inter-zygapophyseal length; and LW, lamina width.

weighted most heavily in one of the first six principal components (see supplementary material Table S3). A second stepwise linear regression using this subset of measurements predicted stiffness in dorsal extension (R^2=0.279) by lamina width (P=0.0078) and centrum height (P=0.0136); stiffness in lateral flexion (R^2=0.520) by lamina width (P=0.0051), neural spine angle (P<0.0001) and centrum width (P=0.0068); and stiffness in ventral flexion (R^2=0.335) by centrum height (P=0.0490) and neural spine angle (P=0.0003) (Table 3).

Experimental design

We examined the experimental design and found no reason to suspect that methodological errors made any qualitative difference to our results. The estimated standard error of digitization, calculated by digitizing a single random image 10 times, was 0.013 deg of angular deflection, compared with an average of 0.12 deg of deflection produced by loading it with the smallest mass (0.01 kg), which indicates that the digitization process was highly repeatable. The regression lines used to approximate stiffness fitted the displacement curves very well: only four out of 165 cases had adjusted R^2 values below 0.75, and those cases were excluded from the analysis. An additional 11 cases were excluded because the P-value of the regression line was >0.05. Not counting specimen 8, a total of 19 out of 168 possible stiffness measurements were excluded (Table 4).

The stiffness of a single vertebra (i.e. the entire bony structure) was ~20 times the stiffness of a representative cranial (T4–5) or caudal (T7–8) intact joint (see supplementary material Fig. S1). Thus, we estimate that the actual joint stiffness is about 10% higher than the reported value because deformation of the two vertebral bodies contributed somewhat to deflection of the pins. However, this calculation does not take into account variation in torque along the vertebral segment, which might make both our estimation of vertebral deformation and the actual joint stiffness marginally higher. Exclusion of the two most cranial joints from specimen 7, which corresponded to different vertebral numbers from those in other specimens, did not result in any change in the stiffness patterns or statistical results. The greatest source of error

The Journal of Experimental Biology (2014) doi:10.1242/jeb.089904

Table 2. Correlations between morphometrics and stiffness in each bending direction

	Dorsal (51)	Lateral (44)	Ventral (51)
PZA	0.265	0.404**	0.244
TPAD	0.468**	0.595**	0.385**
TPAC	0.045	−0.088	−0.014
NSA	–0.444**	–0.600**	–0.512**
NSL	0.176	0.354*	0.119
CL	0.198	0.298*	0.256
CW	0.239	0.129	0.076
NSH	0.019	–0.301*	−0.066
CH	0.370**	0.218	0.298*
PZW	0.599**	0.592**	0.407**
IZL	0.314*	0.300*	0.294*
TPW	0.136	0.285	0.181
TPLT	0.009	0.180	0.092
LW	0.375**	0.396**	0.161

Values are Pearson correlation coefficients. The number of cases is shown in parentheses.

Asterisks indicate significant correlations (*P<0.05) and highly significant correlations (*P<0.001).

PZA, pre-zygapophyseal angle; TPAD, dorsoventral transverse process angle; TPAC, craniocaudal transverse process angle; NSA, neural spine angle; NSL, neural spine length; CL, centrum length; CW, centrum width; NSH, neural spine height; CH, centrum height; PZW, pre-zygapophyseal width; IZL, inter-zygapophyseal length; TPW, transverse process width; TPLT, transverse process length at tip; and LW, lamina width.

was variation between trials, with a small but significant increase in stiffness between the first and second trials (1.9% of mean normalized stiffness in trial 1; P=0.0030) and between the first and third trials (3.3% of mean normalized stiffness in trial 1; P<0.0001) (see supplementary material Table S4). This effect may be a product of an increase in the neutral zone due to tissue fatigue; however, it should not affect our interpretation because only the first trial was used in subsequent statistical analyses.

DISCUSSION

We measured passive intervertebral joint stiffness in three bending directions throughout the thoracolumbar vertebral column of *C. niloticus* to investigate patterns of stiffness and their relationship to vertebral morphology. The intervertebral joints were somewhat stiffer in dorsoventral versus mediolateral bending, except at the lumbosacral joint where mediolateral stiffness was the highest. Joint stiffness increased caudally along the column, particularly in mediolateral bending. Counter-intuitively, severing intervertebral ligaments resulted in a small increase in stiffness, probably as a result of the greater joint excursion angles reached at small weight increments (increase in neutral zone). Several morphometric measurements were correlated with stiffness in ways that agreed with our predictions, as described below.

Implications of joint stiffness for crocodylian locomotor biomechanics

Like mammals, crocodylians use some degree of axial movement across many modes of locomotion. Kinematic studies reveal moderate mediolateral pelvic/sacral rotations (10–15 deg) during high walk and sprawling locomotion in alligators (Gatesy, 1991; Reilly and Elias, 1998), slight lateral undulations of the body in some types of swimming (Frey and Salisbury, 2001), and speed-dependent dorsoventral movements of the pre-sacral column during bounding and galloping (Renous et al., 2002). However, intervertebral joint angles and the contributions of different regions of the vertebral column to locomotor dynamics are unknown. Our results show that the patterns of joint stiffness for *C. niloticus* are different from those reported for mammalian vertebral mechanics, suggesting that the mechanical role of the vertebral column also is different between the two groups. This difference is not surprising, because crocodylian and mammalian lineages have evolved independently for ~320 million years. Nonetheless, because some crocodylians use analogous asymmetrical gaits, it might have been expected that they would exhibit similar patterns of dorsoventral stiffness, particularly at the lumbosacral joint.

Variation in dorsoventral stiffness along the vertebral column

In the mammalian vertebral column, dorsoventral stiffness is closely tied to locomotor function. Dorsoventral movements of the lumbar region are considered to be important for increasing step length and the speed of the swing leg in asymmetrical gaits (Hildebrand, 1959), and patterns of dorsoventral stiffness mirror patterns of joint flexion/extension during locomotion. In agreement with biomechanical studies showing the lumbosacral joint in several terrestrial mammals to have relatively low dorsoventral stiffness and high mobility (e.g. Gál, 1993a; Jeffcott and Dalin, 1980; Slijper, 1946), kinematic studies have shown that the

Table 3. Morphological predictors of joint stiffness for each bending direction by stepwise linear regression

Variable	Coefficient	s.e.	s.c.	T	Collinearity	R^2
Dorsal extension (49)						0.279 (<0.0001)
Lamina width	0.155	0.056	0.353	2.782 (0.0078)	0.954	
Centrum height	0.313	0.122	0.325	2.565 (0.0136)	0.954	
Lateral flexion (44)						0.520 (<0.0001)
Neural spine angle	−0.030	0.005	−0.602	−5.904 (<0.0001)	0.950	
Centrum width	0.162	0.031	0.619	5.265 (<0.0001)	0.930	
Lamina width	0.180	0.040	0.542	4.532 (0.0001)	0.941	
Ventral flexion (50)						0.335 (<0.0001)
Centrum height	0.207	0.103	0.245	2.020 (0.0490)	0.941	
Neural spine angle	–0.018	0.005	–0.468	−3.860 (0.0003)	0.941	

The stepwise linear regression was performed using a subset of the morphological parameters identified by principal components analysis (see 'Statistical analysis' section of Materials and methods).

s.c., standardised coefficient; R^2, coefficient of determination. Sample size is given in parentheses after each variable.

Regression equation: y_i=β0+β1$x1_i$+β2$x2_i$+ ... +β$px p_i$+e_i (see Materials and methods for details). Constants (β) were −7.953 for the dorsal extension equation, −3.951 for the lateral flexion equation and −3.677 for the ventral flexion equation.

Collinearity is the tolerance, i.e. the proportion of variation that cannot be accounted for by other factors.

P-values are indicated in parentheses to the right of each value of T and R^2.

greatest dorsoventral bending amplitude tends to occur at the lumbosacral joint (e.g. Haussler et al., 2001; Hildebrand, 1959; Nyakatura and Fischer, 2010; Schilling and Hackert, 2006; Slijper, 1946). In contrast, stiffness in all bending directions in *C. niloticus* increased with craniocaudal position and was highest at the lumbosacral joint (Fig. 1), suggesting that bounding and galloping crocodiles would need to generate very large moments about this joint to produce an appreciable degree of flexion/extension. If the relationship between passive joint stiffness and kinematics that has been observed in mammals also applies to crocodylians, it follows that crocodiles must either rely less upon axial dorsoventral flexion during asymmetrical gaits than mammals do, or distribute the bending more evenly across the trunk. This high stiffness is likely to be useful in supporting their large tails and countering hindlimb forces, which are proportionately greater in crocodilians (Willey et al., 2004).

Variation in mediolateral stiffness along the vertebral column

The trend of increasing intervertebral joint stiffness in a craniocaudal direction is most pronounced in the mediolateral direction (Fig. 1). This result was unexpected, because the few studies of regional vertebral motion during locomotion in non-mammalian tetrapods show the greatest mediolateral flexion occurring in the caudal-most region in trotting lizards (Ritter, 1995) and salamanders (O'Reilly et al., 2000). However, regional axial flexion (either dorsoventral or mediolateral) has not been studied in crocodylians, and they may show a different pattern. Likewise, passive joint stiffness has not been measured in lizards or salamanders. It is even possible that the increased mediolateral stiffness may stabilize the lumbosacral joint against lateral movements during asymmetrical gaits, constraining it to move predominantly in the dorsoventral plane.

Alternatively, the high joint stiffness might indicate higher forces rather than smaller degrees of flexion. It has been suggested that crocodylians experience particularly high craniocaudal shear forces in the lumbosacral region because of the action of epaxial muscles (Salisbury and Frey, 2000), which could be balanced by high stiffness in this region. The osteoderms, which comprise more rows in the mid-thoracic region than in the lumbar region (Ross and Mayer, 1983), and the ribcage likely stiffen the thoracic region and may compensate for the lower stiffness of intervertebral joints, and/or the thoracic region might be stabilized by axial muscles. Finally, the high mediolateral stiffness of the lumbosacral joint might serve to absorb and propagate forces generated by the hindlimbs during terrestrial locomotion (Reilly et al., 2006) or moments generated by undulation of the tail, which is the primary source of thrust in swimming (Fish, 1984; Frey and Salisbury, 2001). Among aquatic mammals, dolphins, which also use tail propulsion for swimming, show increased stiffness in the lumbosacral joints (Long et al., 1997), while phocid seals, which use hindlimb propulsion, do not (Gál, 1993a).

Variation in stiffness between bending directions

We also observed departures from the general mammalian pattern in relative stiffness in different bending directions. Joint stiffness was significantly lower in lateral flexion than in dorsoventral flexion, though there was no significant difference between stiffness in dorsal extension versus ventral flexion (Table 1B). In contrast, equine vertebral columns are stiffer in mediolateral bending than in dorsoventral bending (Schlacher et al., 2004), and a wide range of mammals have vertebral columns that are significantly stiffer in dorsal extension than ventral flexion (e.g. Gál, 1993a; Gaudin and Biewener, 1992; Jeffcott and Dalin, 1980; Long et al., 1997). Lower mediolateral stiffness in crocodiles was expected because crocodiles employ substantial lateral flexion of the trunk during symmetrical gaits (Reilly and Elias, 1998) and a small amount during swimming (Fish, 1984; Frey and Salisbury, 2001). Uniformly high stiffness in ventral flexion might confer an advantage for crocodylians in terms of passive maintenance of posture. Crocodylians habitually maintain a dorsally convex arch of the vertebral column by contraction of the abdominal and other axial muscles, generating a moment that tends to flex the vertebral column ventrally (that is, increase the dorsal convexity) (Frey, 1988). The metabolic cost of maintaining this posture could be reduced by resisting this moment through intervertebral joint stiffness rather than epaxial muscle contraction.

Vertebral morphology and stiffness

Regional differentiation in the crocodilian vertebral column is not as pronounced as seen in mammals (Pierce et al., 2011; Slijper, 1946). However, changes in vertebral morphology were evident around T4–T5 (cranial versus caudal thoracic), L1–L2 (caudal thoracic and first lumbar versus remaining lumbar) and L5–S1 (lumbar versus sacral) (Fig. 2). Pre-zygapophyseal angle was always greater than 90 deg and increased slightly throughout the thoracic column, and neural spine inclination shifted gradually from caudal to vertical. Crocodylians do not display a diaphragmatic or anticlinal vertebra, which may explain why we failed to observe some correlations between morphometrics and stiffness that have been documented in mammals, as explained below.

Utility of prediction models

Some, but not all, of our predictions regarding the relationship between vertebral dimensions and stiffness in *C. niloticus* (see 'Morphological parameters' in Materials and methods) were borne out by our analysis. The following hypotheses were supported: (1) stiffness in dorsal extension and ventral flexion was correlated positively with centrum height, and stiffness in dorsal extension was correlated positively with lamina width (Table 2); (2) stiffness in lateral flexion was correlated positively with distance between pre-zygapophyses (Table 2), and centrum width contributed significantly to the prediction model with a positive coefficient (Table 3).

Centrum width was not significantly correlated with mediolateral stiffness, but it was included in the prediction model because it significantly improved the model fit in combination with other measurements. Measurements that were significantly correlated with stiffness, but were not included in the prediction model, such as pre-zygapophyseal width, were highly correlated with other measurements that were included in the model (see supplementary material Table S1).

Our stepwise linear regression prediction models using a subset of morphometric measurements accounted for 28–52% of the variation in stiffness ($0.279<R^2<0.520$) (Table 3). While this result means that ~48–72% of stiffness variation remains unaccounted for, it does not mean that morphology is a poor indicator of stiffness. To reduce multicollinearity and make the prediction models easier for others to use, we only included two to four measurements in each model. A principal components regression using all measurements accounted for 34–82% of the variation (see supplementary material Table S2). The remaining proportion of variation may be explained by variation in properties of the ligaments and joint capsules, and the shape and area of articular surfaces (along with experimental error). Compared with lateral flexion, stiffness in dorsal extension and ventral flexion varied less along the column, which may account

The Journal of Experimental Biology (2014) doi:10.1242/jeb.089904

for their weaker correlations with morphometric measurements. Also, vertebral morphology might be a more powerful indicator of stiffness across genera and species than within one species of *Crocodylus*.

Individual morphometric measurements

Vertebral centra are the primary structures that resist compressive axial forces, and the relationship between dimensions of the centra and stiffness has long been described using beam theory (e.g. Christian and Preuschoft, 1996; Slijper, 1946). Dorsoventrally flattened centra are understood to increase sagittal flexibility by decreasing the moment of resistance in the dorsoventral plane, permitting the dorsoventral motion that characterizes terrestrial locomotion in mammals (Boszczyk et al., 2001; Shapiro, 2007). Spool-shaped centra with a high ratio of length to cross-sectional area are thought to allow greater flexibility than more axially compressed vertebral bodies (Buchholtz, 2001), while relatively short centra promote stability by decreasing bending moments and increasing joint contact area (Pierce et al., 2011; Shapiro, 2007). In line with our initial predictions, we found that an increase in centrum height was significantly correlated with an increase in joint stiffness in dorsal extension and ventral flexion (Table 2) and was a significant predictor of stiffness in both directions, whereas centrum width was a significant predictor of mediolateral stiffness (Table 3). Thus, increases in centrum diameter may be an important mechanism for stiffening the lumbosacral region in crocodylians. Contrary to our predictions and to the results of a similar study on dolphins (Long et al., 1997), centrum length showed either a positive correlation or no correlation with stiffness. This result may simply reflect the relatively small change in centrum length along the vertebral column in *C. niloticus* (Fig. 2).

Zygapophyseal orientation is considered by many authors to be one of the best osteological clues to axial flexibility and function because the close contact between zygapophyses constrains the range and direction of movement of the intervertebral joint (Holmes, 1989; Pierce et al., 2011). It is widely accepted that more horizontally oriented pre-zygapophyses (>90 deg) permit greater mediolateral flexion, whereas more vertically oriented ones (<90 deg) permit greater dorsoventral flexion (Boszczyk et al., 2001; Finch and Freedman, 1986; Hua, 2003). Wider mediolateral spacing of pre-zygapophyses is thought to increase joint stability (Boszczyk et al., 2001; Holmes, 1989) and craniocaudal distance between zygapophyses may increase dorsoventral range of motion (Shapiro, 2007). Our results showed significant correlation of pre-zygapophyseal angle only with increased mediolateral stiffness, suggesting that it is not an important determinant of dorsoventral stiffness in crocodiles. However, like centrum length, pre-zygapophyseal angle did not vary greatly along the column (Fig. 2), and so this result should not be overstated. In contrast, mediolateral spacing of the pre-zygapophyses was highly correlated with stiffness in all directions (Table 2). It was also highly correlated with lamina width, an important predictor of stiffness in dorsal extension and lateral flexion in mammals (Shapiro, 2007) (Table 3). In combination, wider laminae and greater mediolateral spacing of pre-zygapophyses appear to increase the stiffness of the crocodylian vertebral column in both the mediolateral and dorsoventral planes.

The lengths of vertebral processes (neural spines and transverse processes) affect axial bending by determining the leverage of muscles that flex and extend the vertebral column, with longer processes being associated with more powerful active extension of intervertebral joints (Frey, 1988; Pierce et al., 2011; Shapiro et al., 2005; Slijper, 1946). Longer vertebral processes also provide greater areas of attachment and leverage for intervertebral ligaments and encompass larger axial musculature, which increases passive stiffness (Valentin et al., 2012). Long et al. (Long et al., 1997) proposed that very stiff intervertebral joints were likely to have wide transverse processes, although they admitted that the relationship between transverse process width and stiffness was not explained by their results. We recorded marked variation in transverse process width and neural spine height along the vertebral column in *C. niloticus* (Fig. 2); however, neither of these was correlated with stiffness in any direction (except for neural spine width and height in lateral flexion, probably as a result of their high correlation with other factors), nor did either contribute to the prediction models. This lack of correlation might have been caused by the use of isolated vertebral columns devoid of muscles and tendons. Because back stiffness can be much greater in live animals than in excised vertebral columns (Ritruechai et al., 2008), moment arms of vertebral processes may be more important for predicting dynamic rather than passive stiffness. As we did not examine live animals and we removed the axial musculature prior to testing, this effect could not be evaluated.

The angles of vertebral processes also affect muscular leverage, and some authors have suggested that they affect joint stiffness and range of motion as well; transverse processes that are oriented more cranially and ventrally are postulated to increase sagittal plane mobility, as are longer and more cranially deflected neural spines (Jeffcott and Dalin, 1980; Shapiro, 2007; Slijper, 1946). Unexpectedly, we obtained the opposite result: ventral deflection of the transverse processes was positively correlated with stiffness, and caudal deflection of the neural spines was negatively correlated with stiffness (Table 2). This result may reflect another difference from many mammals; crocodylian neural spines are never cranially deflected, so an increase in cranial deflection is actually an approach to a vertical orientation. These two measurements also were highly correlated with each other, so it was not clear which, if either, had a direct effect upon joint stiffness.

Effect of severing intervertebral ligaments

Severing the intervertebral ligaments (inter-spinous and inter-transverse) resulted in a small but significant increase in joint stiffness, in contrast to its effect on the intervertebral joints of dolphins (Long et al., 1997). A similar effect was observed in repeated trials on the same joint without severing ligaments (see supplementary material Table S4). The most likely reason for this counter-intuitive result was an increase in the neutral zone of about 1.5 deg due to tissue fatigue. It appears that these ligaments may operate within a limited range of forces that were too small to be detected by our methods. Beyond that range, increases in joint stiffness may be governed by other vertebral structures, such as zygapophyseal capsules. Another potential influence on stiffness to consider is that the water used to hydrate the joints between trials may have caused connective tissue to swell (e.g. around zygapophyseal joint capsules), resulting in an increase in stiffness over repeated trials.

Conclusions

This study is the first to quantitatively examine stiffness of crocodylian intervertebral joints, and the first to rigorously test whether it can be predicted by morphometric measurements. Patterns of intervertebral joint stiffness in crocodiles differ from those reported for mammals both along the column and between bending directions. The contrasting patterns imply that crocodylians have either a different relationship between joint stiffness and axial bending or a different role

The Journal of Experimental Biology (2014) doi:10.1242/jeb.089904

Table 4. Attributes and loading conditions of cadaveric specimens

	Specimen ID								
	1	2	3	4	5	6	7	8	Average
Body mass (kg)	1.375	1.625	2.175	3.2	4.6	6.8	10.1	15.6	5.7
Thoracolumbar length (m)	0.135	0.132	0.149	0.189	0.233	0.214	0.287	0.318	0.207
Max. applied mass (kg)	0.70	0.70	0.70	0.80	1.20	1.00	1.50	1.00	0.95
Number of increments	12	12	13	10	18	12	17	14	13.5
Cases analysed	13	23	24	24	23	24	18	0	18.6
Tests with ligaments cut	No	No	No	Yes	No	Yes	No	Yes	

Thoracolumbar length was approximated by summed centrum length taken from isolated vertebrae.
The maximum applied mass and number of increments refer to the metric weights applied to the joint during stiffness testing.
The number of cases analysed is the number of stiffness measurements out of a possible 24 that were used in the final analysis (see 'Experimental design' in Results for inclusion criteria).

for the axial column during locomotion, even within similar gaits. Some, but not all, of our predictions regarding the relationship between vertebral dimensions and joint stiffness in *C. niloticus* were borne out in our analysis, indicating a complex relationship between bony morphology and the surrounding soft tissue. Nonetheless, this study represents a key step towards understanding the functional role of the vertebral column in crocodylian locomotion, from which broader evolutionary questions can be addressed.

MATERIALS AND METHODS

Specimens and joint preparation

We excised and examined eight vertebral columns from cadaveric specimens of juvenile Nile crocodiles (*C. niloticus*) with body masses ranging from 1.3 to 15.6 kg (Table 4). The animals, provided by conservation centre La Ferme aux Crocodiles (Pierrelatte, France), had died of natural causes and were sealed in airtight plastic bags and frozen immediately thereafter. They were thawed at room temperature for ~24 h before dissection. Only the thoracic and lumbar vertebrae were tested because their primary function is body support and body mobilization during terrestrial locomotion. Cervical morphology is likely to be influenced by the requirements of feeding, and caudal morphology by the requirements for swimming, although the thoracolumbar column also contributes to some types of swimming (Frey and Salisbury, 2001). Following excision, the thoracolumbar region of the vertebral column was divided into eight segments (Fig. 3), each consisting of two vertebrae (i.e. one intervertebral joint) and the intervening intact ligaments and joint capsule. The segments were immediately enclosed in airtight plastic bags and re-frozen.

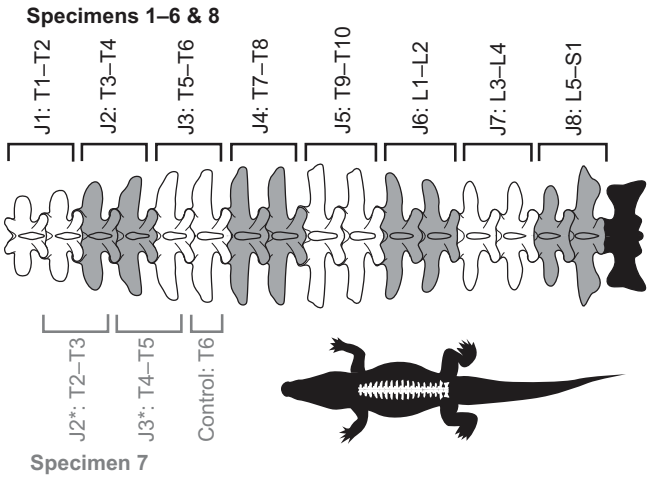

Fig. 3. Thoracolumbar vertebral column of *C. niloticus*, illustrating the joints tested in passive stiffness experiments. In specimens 1–6 and 8, the thoracolumbar column was divided into eight joints (J1–J8; two vertebrae per joint). In specimen 7, J1 was omitted (hence J2 and J3 are defined differently as indicated by asterisks) and the sixth thoracic vertebra was tested in isolation.

Before an experiment was run, each joint segment was thawed at room temperature for 1–4 h, depending on the size of the specimen. Small holes were drilled into the centres of the vertebral centra: one on the cranial aspect of the cranial-most vertebra, and one on the caudal aspect of the caudal-most vertebra, and wood screws were inserted. Drill bits and screws were carefully measured and marked so that they penetrated ~2/3 of the centrum while stopping well short of the joint capsule. Each joint was X-rayed to confirm that the screws were in the proper positions. Finally, pins were anchored in the neural spine and right transverse process of each vertebra to aid in visually tracking the positions and angles of the vertebrae over the course of the experiment (Fig. 4A). Joint segments were kept moist with water throughout the experiments.

Recording joint deflection

The cranial-most screw was clamped to immobilize one vertebra in each pair while leaving the other free to move around the joint, similar to Long et al. (Long et al., 1997). Change in intervertebral joint angle was recorded using high-resolution photography, provided by a tripod-mounted camera with a zoom lens set to 107 mm. To minimize optical distortion, the height, angle and position of the tripod head were adjusted so that the lens was aimed in a horizontal plane perpendicular to the long axis of the vertebrae and the intervertebral joint was in the centre of the field of view. At the beginning of each round of testing, the unloaded joint was photographed with a spirit level marked in centimetre increments. This reference image allowed us to calculate initial joint angle, scale and orientation with respect to gravity (Fig. 4A).

Each joint was loaded with metric weights suspended from the head of the screw in the caudal-most vertebra. The exact weights used were adjusted based upon the size of the specimen, but each joint was loaded with a minimum of 10 different weights (Table 4). Between measurements, the joint was unloaded and returned to an approximately neutral position by gently nudging it back into place.

For all joints in three of the specimens, the experiment was repeated after the ligaments between the neural spines and transverse processes had been severed (in ventral flexion and lateral flexion only). The same specimens were used to test both ventral flexion and lateral flexion, but the order of the tests was varied so that we could assess whether severing interspinous ligaments affected mediolateral stiffness or vice versa; no such effects were detected. This test was used to assess the contribution of intervertebral ligaments to joint stiffness. Repeatability and the effect of fatigue induced by repeated loading of the joint were examined for all joints in three specimens by repeating the loading experiment two or three times with the ligaments intact. Because vertebrae of juvenile crocodiles might not behave as true rigid bodies, an additional test was performed to quantify the change in angle caused by deformation of the vertebral bodies rather than flexion/extension of the joint. The sixth thoracic vertebra from specimen 7 was isolated, drilled and loaded in the same manner as the joints had been.

Eight reference points on the vertebrae, pins and screws were digitized from each photograph in ImageJ software (http://rsbweb.nih.gov/ij) to track displacement of the vertebrae under load. An additional four points were

The Journal of Experimental Biology (2014) doi:10.1242/jeb.089904

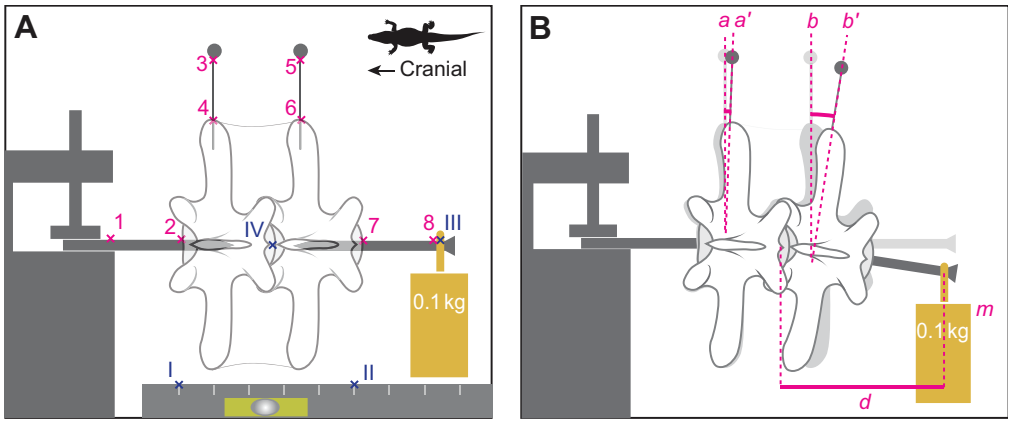

Fig. 4. Experimental setup for testing passive mediolateral stiffness and the procedure for measuring angular deflection of the joint. (A) The cranial-most vertebra was immobilized, while the caudal-most vertebra was allowed to move freely about the intervening joint. Metric weights were suspended from a screw inserted in the centrum of the caudal-most vertebra, and the resulting deflection angles were recorded using high-resolution photography. Four reference points were digitized on a photograph in the initial unloaded condition to record scale and direction of gravity (I and II) and initial moment arm of the weight (III and IV). Eight further points (1–8) were digitized on multiple images covering a range of weight increments to record changes in angular deflection of the cranial-most and caudal-most vertebrae. (B) Joint deflection was calculated by subtracting the change in vector of the cranial-most pin in the unloaded (*a*) and loaded (*a′*) condition from that of the caudal-most pin (*b*–*b′*). Applied moment was calculated by multiplying the mass of the metric weight (*m*; in kg) by the gravitational constant (9.81 m s^{-2}) and the distance between the application of force and the centre of rotation (*d*).

digitized from the initial unloaded image to calculate scale and orientation with respect to gravity. Observer error was quantified by digitizing all points on a single randomly chosen photograph 10 times and reporting the standard deviation of the calculated deflection angles.

Determining stiffness

A script was custom-written in MatLab software (MathWorks Inc., Natick, MA, USA) to calculate angular deflection and applied bending moment. Angular deflection in degrees was derived from digitized points on the photographs using the following equation:

$$\Delta\theta = (b - a) - (b' - a') \ , \quad (1)$$

where deflection ($\Delta\theta$) is the difference between the initial pin angles, a and b, determined by the points digitized on the cranial and caudal pins (3–4 and 5–6 in Fig. 4A, respectively) in the initial reference photograph, and the pin angles in the loaded condition, a' and b', determined by the same points on the loaded photograph (Fig. 4B).

The applied bending moment (**M**) was calculated from digitized points on the photographs and the known mass of the metric weights:

$$\mathbf{M} = m_{\mathrm{w}} \times \boldsymbol{g} \times \mathrm{d} \ , \quad (2)$$

where m_{w} is the mass of the weights in kilograms, $\boldsymbol{g}$ is gravitational acceleration (9.81 m s^{-2}) and d is the horizontal distance in metres (i.e. perpendicular to the weight action) between the centre of rotation (estimated as the middle of the intervertebral joint in the photographs) and the attachment of the weights (moment arm); d was calculated during the experiment from each 'loaded' photograph (Fig. 4B). The raw data (deflections versus non-normalized moments) are available in supplementary material Table S5).

Stiffness was calculated by taking the linear regression of normalized moment versus angular deflection over a small initial range of moments. Moments were normalized based on geometric similarity theory (Hof, 1996) by dividing by the product of specimen mass and thoracolumbar length (approximated by summed centrum length). The slopes of the regression lines were then log-transformed to normalize their distribution. The range of moments used to determine the slope was defined by the approximate linear region of the graph, covering a small initial range of values (e.g. Ianuzzi et al., 2009; Long et al., 1997; Schlacher et al., 2004); in this case, <0.1 normalized moment, which corresponds to ~0.15 N m in a 4.6 kg specimen (Fig. 5). The first weight increment was excluded because it includes the neutral zone, i.e. the presumed range of angles over which the joint can move without the application of force (Panjabi, 1992). Cases were excluded from the analysis if the regression lines had P>0.05 or R^2<0.75.

Morphological parameters

After the stiffness experiment, the excised joints were cleaned of all soft tissue, and 10 linear and four angular measurements were taken from each vertebra

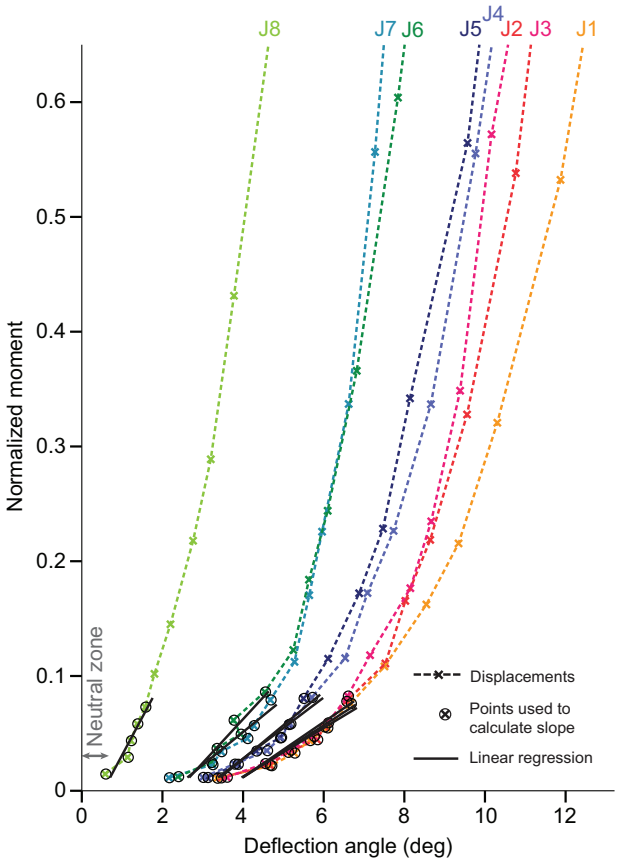

Fig. 5. Representative graph of normalized moment plotted against angular joint deflection (mediolateral) for all joints (specimen 3). Angular displacement was calculated for 13 different moments, and best-fit regression lines were calculated from the points within the estimated linear range of the resulting curve (<0.1 normalized moment). Stiffness was defined as the slope of the regression line.

The Journal of Experimental Biology (2014) doi:10.1242/jeb.089904

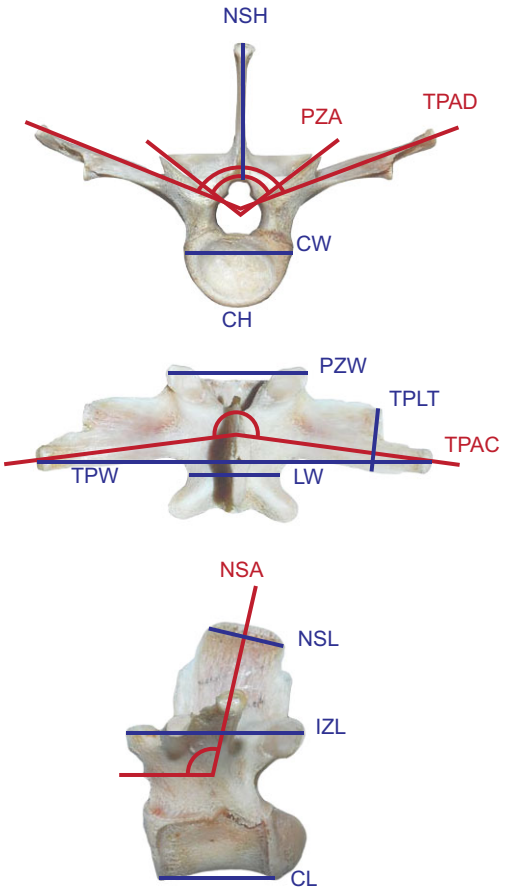

Fig. 6. Linear and angular morphometric measurements taken from vertebrae. All lengths are craniocaudal, all widths are mediolateral, and all heights are dorsoventral. Linear measurements (in millimetres) were centrum length (CL), centrum width (CW), centrum height (CH), neural spine length (NSL), neural spine height (NSH), transverse process width (TPW), transverse process length at tip (TPLT), pre-zygapophyseal width (PZW), inter-zygapophyseal length (IZL) and lamina width (LW). Angular measurements (deg) were pre-zygapophyseal angle (PZA), neural spine angle (NSA), dorsoventral transverse process angle (TPAD) and craniocaudal transverse process angle (TPAC).

(Fig. 6). These measurements had been correlated with mechanical properties and/or locomotor behaviour in previous studies (Boszczyk et al., 2001; Buchholtz, 2007; Hebrank et al., 1990; Hua, 2003; Long, 1992; Long et al., 1997; Pierce et al., 2011; Shapiro, 2007). Linear measurements were taken with digital callipers, and angular measurements were taken from digital photographs in ImageJ. Prior to statistical analysis, linear measurements were normalized using the statistics package PAST (Hammer et al., 2001), version 2.15 (http://folk.uio.no/ohammer/past) using the allometric scaling function:

$$M_{\mathrm{n}} = M\left(\frac{L_{\mathrm{s}}}{L_{\mathrm{o}}}\right)^{b}, \qquad (3)$$

where M_{n} is the normalized measurement, M is the original measurement, L_{s} is overall mean thoracolumbar length for all specimens (approximated by summing centrum length from each of the 16 thoracolumbar vertebrae), L_{o} is thoracolumbar length of the current specimen, and b is the slope of the regression of $\log_{10}M$ on $\log_{10}L_{\mathrm{o}}$ for each measurement, using all specimens (Pierce et al., 2011). Non-normalized morphometrics are included in supplementary material Table S6.

Based upon previous studies of intervertebral joint stiffness and locomotion cited in the Introduction, we made the following predictions about how the various morphometric measurements would relate to stiffness in different bending directions (see Discussion): (1) stiffness in dorsal extension and ventral flexion is expected to correlate positively with centrum height, neural spine length and height, caudal deflection of the neural spine, pre-zygapophyseal angle, dorsal and caudal deflection of the transverse processes, and lamina width; (2) stiffness in dorsal extension and ventral flexion is expected to correlate negatively with centrum length and craniocaudal spacing of the zygapophyses; (3) stiffness in lateral flexion is expected to correlate positively with centrum width, transverse process width, and distance between pre-zygapophyses; and (4) stiffness in lateral flexion is expected to correlate negatively with pre-zygapophyseal angle.

Statistical analyses

Variation in intervertebral joint stiffness was examined by joint number and bending direction to determine whether stiffness changed along the vertebral column and whether the column was stiffer in different bending directions. This analysis used a two-way ANOVA with normalized stiffness as the dependent variable and joint (J1–J8) and bending direction (ventral flexion, dorsal extension, lateral flexion) as the independent variables. *Post hoc* pair-wise comparison tests (with a Bonferroni correction) were conducted to identify which groups were significantly different. The effects of severing intervertebral ligaments and multiple trials on joint stiffness were examined using repeated-measures ANOVA.

To determine which morphological parameters were the best predictors of joint stiffness, we first looked at Pearson's correlations between all 14 normalized morphometric measurements and normalized stiffness in each bending direction. Next, we conducted a stepwise linear regression for each bending direction using all morphometric measurements as independent variables, similar to a previous study (Long et al., 1997). However, the regression models displayed potential problems with multi-collinearity, making it difficult to confidently determine which morphometric measurements were contributing to the regression model.

To address this problem, we performed a principal components analysis to generate a set of uncorrelated factors. Then, a second stepwise linear regression was conducted using only those morphometric parameters weighted most heavily in one of the first six principal components, which accounted for >90% of the variance in the morphometrics data. We chose this method rather than a principal components regression because the principal components are not directly comparable to anatomical measurements. For each bending direction, the model reported was the one that had the highest R^2 value and where tolerances (a measure of non-collinearity) of all factors were greater than 0.6. All statistical analyses were conducted in IBM SPSS version 20 (http://www-01.ibm.com/software/analytics/spss/) and assessed at a significance level of $P<0.05$.

Some values were missing or excluded from the analyses. Specimen 8 was excluded from stiffness calculations (but not from severed ligament tests) because the moments used did not cover the full range needed to calculate stiffness. Because of the preservation quality of specimen 7, J1 was not measured, and J2–J3 were defined differently: J2 was T2–T3 and J3 was T4–T5 (see Fig. 3). To determine whether this difference affected the statistical results, the analyses were run with and without J2 and J3 from specimen 7. Also excluded was J5 of specimen 2, which was found to be malformed after soft tissue was removed.

Acknowledgements

We thank Samuel Martin, Eric Fernandez and other staff of La Ferme aux Crocodiles (Pierrelatte, France) for providing the cadaveric specimens. Phil Pickering is gratefully acknowledged for his technical assistance with the experimental apparatus design, setup and data collection, as well as analysis code. Richard Prior and staff of the post-mortem facility at The Royal Veterinary College assisted with dissections and facility access. We thank Vivian Allen, Stephen Amos, Luis Lamas, Michael Pittman, Emily Sparkes and Renate Weller for discussions and other assistance with this study, and Ruby Chang, Heather Paxton and Simon Wilshin for advice on statistical analyses. Finally, we thank our two anonymous reviewers, whose helpful suggestions greatly improved this manuscript.

Competing interests

The authors declare no competing financial interests.

Author contributions

Concepts and approach were developed by J.R.H., S.E.P. and J.L.M. Experiments and data analysis were performed by J.L.M. and S.E.P. The manuscript was prepared by J.L.M. and edited by S.E.P. and J.R.H. prior to submission.

Funding
This study was funded by the Natural Environment Research Council (NERC) [grant no. NE/G005877/1 to J.R.H. and S.E.P.].

Supplementary material
Supplementary material available online at
http://jeb.biologists.org/lookup/suppl/doi:10.1242/jeb.089904/-/DC1

References

Blob, R. W. and Biewener, A. A. (1999). In vivo locomotor strain in the hindlimb bones of *Alligator mississippiensis* and *Iguana iguana*: implications for the evolution of limb bone safety factor and non-sprawling limb posture. *J. Exp. Biol.* **202**, 1023-1046.
Boszczyk, B. M., Boszczyk, A. A. and Putz, R. (2001). Comparative and functional anatomy of the mammalian lumbar spine. *Anat. Rec.* **264**, 157-168.
Buchholtz, E. A. (2001). Vertebral osteology and swimming style in living and fossil whales (Order: Cetacea). *J. Zool. (Lond.)* **253**, 175-190.
Buchholtz, E. A. (2007). Modular evolution of the cetacean vertebral column. *Evol. Dev.* **9**, 278-289.
Carpenter, K. (2009). Role of lateral body bending in crocodylian track making. *Ichnos* **16**, 202-207.
Christian, A. and Preuschoft, H. (1996). Deducing the body posture of extinct large vertebrates from the shape of the vertebral column. *Palaeontology* **39**, 801-812.
Finch, M. E. and Freedman, L. (1986). Functional-morphology of the vertebral column of *Thylacoleo carnifex* Owen (Thylacoleonidae, Marsupialia). *Aust. J. Zool.* **34**, 1-16.
Fish, F. E. (1984). Kinematics of undulatory swimming in the American alligator. *Copeia* **4**, 839-843.
Frey, E. F. (1988). The carrying system of crocodilians – a biomechanical and phylogenetical analysis. *Stuttgarter Beiträge zur Naturkunde, Serie A (Biologie)* **426**, 1-60.
Frey, E. F. and Salisbury, S. W. (2001). The kinematics of aquatic locomotion in *Osteolaemus tetraspis* Cope. In *Crocodilian Biology and Evolution*, pp. 165-179. Baulkham Hills, NSW, Australia: Surrey Beatty & Sons.
Gál, J. M. (1993a). Mammalian spinal biomechanics. I. Static and dynamic mechanical properties of intact intervertebral joints. *J. Exp. Biol.* **174**, 247-280.
Gál, J. M. (1993b). Mammalian spinal biomechanics. II. Intervertebral lesion experiments and mechanisms of bending resistance. *J. Exp. Biol.* **174**, 281-297.
Gál, J. (2002). Mammalian spinal biomechanics: postural support in seated macaques. *J. Exp. Biol.* **205**, 1703-1707.
Gatesy, S. M. (1991). Hind limb movements of the American alligator (*Alligator mississippiensis*) and postural grades. *J. Zool. (Lond.)* **224**, 577-588.
Gaudin, T. J. and Biewener, A. A. (1992). The functional morphology of xenarthrous vertebrae in the armadillo *Dasypus novemcinctus* (Mammalia, Xenarthra). *J. Morphol.* **214**, 63-81.
Hammer, Ø., Harper, D. A. T. and Ryan, P. D. (2001). PAST: paleontological statistics software package for education and data analysis. *Palaeontologia Electronica* **4**, 1-9.
Haussler, K. K., Bertram, J. E. A., Gellman, K. and Hermanson, J. W. (2001). Segmental in vivo vertebral kinematics at the walk, trot and canter: a preliminary study. *Equine Vet. J. Suppl.* **33**, 160-164.
Hebrank, J. H., Hebrank, M. R., Long, J. H., Jr, Block, B. A. and Wright, S. A. (1990). Backbone mechanics of the blue marlin *Makaira nigricans* (Pisces, Istiophoridae). *J. Exp. Biol.* **148**, 449-459.
Hildebrand, M. (1959). Motions of the running cheetah and horse. *J. Mammal.* **40**, 481-495.
Hof, A. L. (1996). Scaling gait data to body size. *Gait Posture* **4**, 222-223.
Holmes, R. (1989). Functional interpretations of the vertebral structure in paleozoic labyrinthodont amphibians. *Hist. Biol.* **2**, 111-124.
Hua, S. (2003). Locomotion in marine mesosuchians (Crocodylia): the contribution of the 'locomotion profiles'. *Neues Jahrbuch für Geologie und Palaontologie Abhandlungen* **227**, 139-152.
Ianuzzi, A., Pickar, J. G. and Khalsa, P. S. (2009). Determination of torque-limits for human and cat lumbar spine specimens during displacement-controlled physiological motions. *Spine J.* **9**, 77-86.
Jeffcott, L. B. and Dalin, G. (1980). Natural rigaidity of the horse's backbone. *Equine Vet. J.* **12**, 101-108.
Koob, T. and Long, J. H., Jr (2000). The vertebrate body axis: evolution and mechanical function. *Am. Zool.* **40**, 1-18.
Long, J. H., Jr (1992). Stiffness and damping forces in the intervertebral joints of blue marlin (*Makaira nigricans*). *J. Exp. Biol.* **162**, 131-155.
Long, J. H., Jr, Pabst, D. A., Shepherd, W. R. and McLellan, W. A. (1997). Locomotor design of dolphin vertebral columns: bending mechanics and morphology of *Delphinus delphis*. *J. Exp. Biol.* **200**, 65-81.
McHenry, M., Pell, C. and Jr, J. (1995). Mechanical control of swimming speed: stiffness and axial wave form in undulating fish models. *J. Exp. Biol.* **198**, 2293-2305.
Nowroozi, B. N. and Brainerd, E. L. (2013). X-ray motion analysis of the vertebral column during the startle response in striped bass, *Morone saxatilis*. *J. Exp. Biol.* **216**, 2833-2842.
Nyakatura, J. A. and Fischer, M. S. (2010). Functional morphology and three-dimensional kinematics of the thoraco-lumbar region of the spine of the two-toed sloth. *J. Exp. Biol.* **213**, 4278-4290.
O'Reilly, J. C., Summers, A. P. and Ritter, D. A. (2000). The evolution of the functional role of trunk muscles during locomotion in adult amphibians. *Am. Zool.* **40**, 123-135.
Panjabi, M. M. (1992). The stabilizing system of the spine. Part II. Neutral zone and instability hypothesis. *J. Spinal Disord.* **5**, 390-396, discussion 397.
Parrish, J. M. (1987). The origin of crocodilian locomotion. *Paleobiology* **13**, 396-414.
Piechowski, R. and Dzik, J. (2010). The axial skeleton of *Silesaurus opolensis*. *Journal of Vertebrate Paleontology* **30**, 1127-1141.
Pierce, S. E., Clack, J. A. and Hutchinson, J. R. (2011). Comparative axial morphology in pinnipeds and its correlation with aquatic locomotory behaviour. *J. Anat.* **219**, 502-514.
Pittman, M., Gatesy, S. M., Upchurch, P., Goswami, A. and Hutchinson, J. R. (2013). Shake a tail feather: the evolution of the theropod tail into a stiff aerodynamic surface. *PLoS ONE* **8**, e63115.
Reilly, S. M. and Elias, J. A. (1998). Locomotion in alligator mississippiensis: kinematic effects of speed and posture and their relevance to the sprawling-to-erect paradigm. *J. Exp. Biol.* **201**, 2559-2574.
Reilly, S. M., Willey, J. S., Biknevicius, A. R. and Blob, R. W. (2005). Hindlimb function in the alligator: integrating movements, motor patterns, ground reaction forces and bone strain of terrestrial locomotion. *J. Exp. Biol.* **208**, 993-1009.
Reilly, S. M., McElroy, E. J., Andrew Odum, R. and Hornyak, V. A. (2006). Tuataras and salamanders show that walking and running mechanics are ancient features of tetrapod locomotion. *Proc. Soc. Sci.* **273**, 1563-1568.
Renous, S., Gasc, J. P., Bels, V. L. and Wicker, R. (2002). Asymmetrical gaits of juvenile *Crocodylus johnstoni*, galloping Australian crocodiles. *J. Zool. (Lond.)* **256**, 311-325.
Ritruechai, P., Weller, R. and Wakeling, J. M. (2008). Regionalisation of the muscle fascicle architecture in the equine longissimus dorsi muscle. *Equine Vet. J.* **40**, 246-251.
Ritter, D. (1995). Epaxial muscle function during locomotion in a lizard (*Varanus salvator*) and the proposal of a key innovation in the vertebrate axial musculoskeletal system. *J. Exp. Biol.* **198**, 2477-2490.
Ross, F. D. and Mayer, G. C. (1983). On the dorsal armor of the Crocodilia. In *Advances in Herpetology and Evolutionary Biology* (ed. A. G. J. Rhodin and K. Miyata), pp. 305-331. Cambridge, MA: Harvard University Press.
Salisbury, S. W. and Frey, E. F. (2000). A biomechanical transformation model for the evolution of semi-spheroidal articulations between adjoining vertebral bodies in crocodilians. In *Crocodilian Biology and Evolution* (ed. G. C. Grigg, F. Seebacher and C. E. Franklin), pp. 85-134. Baulkham Hills, NSW, Australia: Surrey Beatty & Sons.
Schilling, N. and Hackert, R. (2006). Sagittal spine movements of small therian mammals during asymmetrical gaits. *J. Exp. Biol.* **209**, 3925-3939.
Schlacher, C., Peham, C., Licka, T. and Schobesberger, H. (2004). Determination of the stiffness of the equine spine. *Equine Vet. J.* **36**, 699-702.
Schwarz-Wings, D., Frey, E. F. and Martin, T. (2009). Reconstruction of the bracing system of the trunk and tail in hyposaurine dyrosaurids (Crocodylomorpha; Mesoeucrocodylia). *Journal of Vertebrate Paleontology* **29**, 453-472.
Shapiro, L. J. (2007). Morphological and functional differentiation in the lumbar spine of lorisids and galagids. *Am. J. Primatol.* **69**, 86-102.
Shapiro, L. J., Seiffert, C. V. M., Godfrey, L. R., Jungers, W. L., Simons, E. L. and Randria, G. F. N. (2005). Morphometric analysis of lumbar vertebrae in extinct *Malagasy strepsirrhines*. *Am. J. Phys. Anthropol.* **128**, 823-839.
Slijper, E. J. (1946). Comparative biologic-anatomical investigations on the vertebral column and spinal musculature of mammals. *Verhandelingen der Koninklijke Nederlandsche Akademie van Wetenschappen* **42**, 1-128.
Valentin, S., Grösel, M. and Licka, T. (2012). The presence of long spinal muscles increases stiffness and hysteresis of the caprine spine in-vitro. *J. Biomech.* **45**, 2506-2512.
Willey, J. S., Biknevicius, A. R., Reilly, S. M. and Earls, K. D. (2004). The tale of the tail: limb function and locomotor mechanics in *Alligator mississippiensis*. *J. Exp. Biol.* **207**, 553-563.

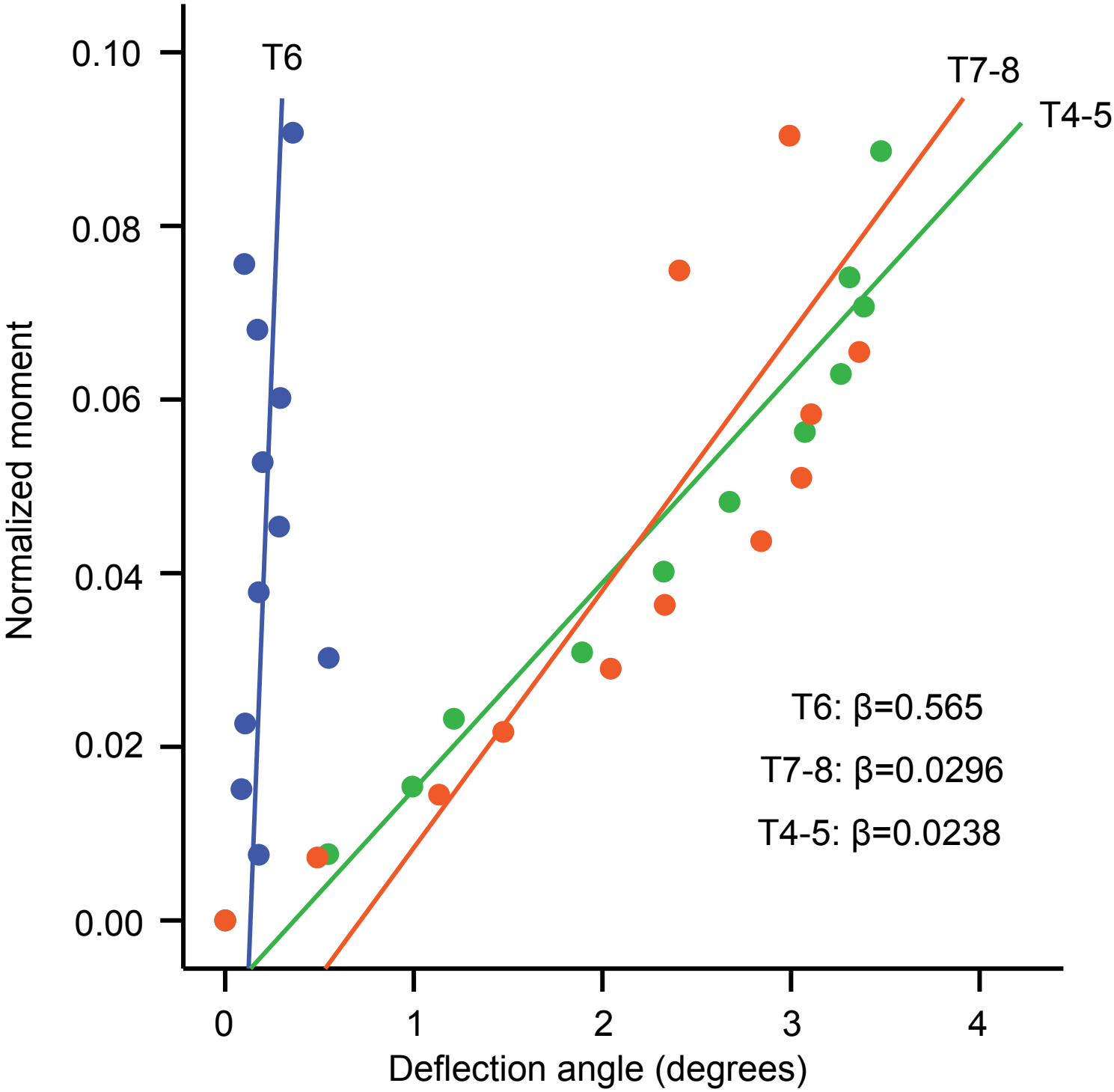

Fig. S1. Stiffness in ventral flexion of a single vertebra compared with craniad and caudad two-vertebra joint complexes (Specimen 7). Normalized moment was plotted against deflection angle in degrees, and stiffness was defined as the slope of the best-fit linear regression (β).

Table S1. Correlations between morphometric measurements

	PZA	TPAD	TPAC	NSA	NSL	CL	NSH	CW	CH	PZW	IZD	TPW	TPLT	LW
PZA	-													
TPAD	.562**	-												
TPAC	-.554**	-.496**	-											
NSA	-.434**	-.665**	.328**	-										
NSL	.519**	.504**	-.577**	-.569**	-									
CL	.491**	.555**	-.523**	-.575**	.778**	-								
NSH	-.368**	-.460**	.459**	.664**	-.685**	-.604**	-							
CW	-.151	.060	.205*	.190*	-.426**	-.491**	.539**	-						
CH	.208*	.280**	-.142	-.171	.137	.188*	.112	.221*	-					
PZW	.631**	.484**	-.316**	-.454**	.564**	.482**	-.352**	-.234**	.382**	-				
IZD	.618**	.474**	-.556**	-.526**	.687**	.684**	-.427**	-.280**	.451**	.676**	-			
TPW	.377**	.450**	-.397**	-.417**	.720**	.702**	-.576**	-.494**	-.122	.414**	.388**	-		
TPLT	-.119	.093	.161	-.147	.333**	.354**	-.339**	-.305**	-.333**	.024	-.053	.688**	-	
LW	.526**	.207*	-.306**	-.148	.411**	.255**	-.280**	-.266**	.186*	.778**	.471**	.240**	-.095	-

Pearson correlations (2-tailed). *Correlation is significant at the 0.05 level, **at the 0.01 level. See text for abbreviations.

Table S2. Stepwise linear regression with all morphometric measurements

			Unstandardized Coefficients		Standardized Coefficients			Collinearity Statistics	
Direction	Model	Factor	B	S.E.	Beta	t	*P*	Tolerance	VIF
Dorsal extension	1	(Constant)	-5.692	.398		-14.315	.000		
		PZW	.112	.022	.599	5.180	.000	1.000	1.000
	2	(Constant)	-6.892	.529		-13.031	.000		
		PZW	.122	.020	.650	6.048	.000	.977	1.024
		CW	.080	.026	.337	3.138	.003	.977	1.024
Lateral flexion	1	(Constant)	-5.360	.310		-17.295	.000		
		TPAD	.009	.002	.595	4.851	.000	1.000	1.000
	2	(Constant)	-9.160	1.068		-8.578	.000		
		TPAD	.014	.002	.945	6.570	.000	**.562**	**1.778**
		TPAC	.016	.004	.529	3.681	.001	**.562**	**1.778**
	3	(Constant)	-10.105	.986		-10.247	.000		
		PZW	.080	.023	.388	3.498	.001	.748	1.338
		TPAD	.011	.002	.748	5.363	.000	**.471**	**2.122**
		TPAC	.016	.004	.527	4.123	.000	**.562**	**1.778**
Ventral flexion	1	(Constant)	-1.759	.440		-3.993	.000		
		NSA	-.020	.005	-.528	-4.352	.000	1.000	1.000
	2	(Constant)	-1.798	.411		-4.372	.000		
		NSA	-.030	.006	-.796	-5.430	.000	**.596**	**1.677**
		NSH	.076	.026	.422	2.878	.006	**.596**	**1.677**

Stepwise linear regression with all morphometrics as independent variables and normalized stiffness as the dependent variable.
Some factors show potential problems with multicollinearity (bold) with tolerances less than 0.6 and variable inflation factors close to 1.

Table S3. Principal components of morphological variation between vertebrae

	1	2	3	4	5	6	7	8	9	10	11	12	13	14
PZA	.487	.259	.328	-.103	.059	.081	.749	-.010	.045	.049	.035	.030	.026	.008
TPAD	.199	.753	.262	.050	-.103	.146	.323	-.137	.035	-.003	.397	.034	.085	.004
TPAC	-.130	-.173	**-.937**	.049	-.100	-.018	-.175	.146	-.088	-.041	-.028	-.026	-.021	-.001
NSA	-.131	**-.941**	-.110	-.102	-.084	-.123	-.047	.159	-.087	-.070	.111	-.020	.003	-.013
NSL	.359	.265	.430	.363	.212	.128	.071	-.227	.593	.099	.011	.046	.051	.008
CL	.270	.390	.390	.295	.458	.207	.174	-.179	.207	.163	.101	.029	.375	.002
CW	-.071	-.003	-.113	-.334	**-.910**	.138	-.018	.131	-.059	-.033	.022	-.025	-.007	-.003
NSH	-.086	-.451	-.285	-.269	-.255	.100	-.016	.738	-.118	-.013	-.026	-.018	-.029	.004
CH	.209	.141	.025	-.177	-.121	**.939**	.045	.049	.035	.040	.017	-.001	.017	.005
PZW	.824	.294	.079	.124	.069	.301	.185	.029	.085	.090	.017	.059	.011	.251
IZD	.456	.324	.434	.031	.234	.388	.146	-.033	.197	.474	-.004	.024	.076	.016
TPW	.298	.231	.392	.620	.326	-.014	.166	-.095	.151	.042	.035	.387	.027	.017
TPLT	.042	.068	-.123	**.907**	.282	-.201	-.110	-.133	.066	-.001	-.002	-.046	.021	.001
LW	**.959**	.037	.130	.075	.060	.071	.127	-.094	.069	.011	.022	.004	.030	-.131

Rotated principal component matrix; rotation method: Varimax with Kaiser Normalization.
Numbers 1-14 represent principal components ordered by the amount of morphological variation for which each accounts. Each component is related to the morphometric measurements to a greater or lesser extent; e.g. lamina width (LW) is heavily weighted in component 1.
Measurements identified for use in subsequent analyses shown in bold. See text for abbreviations.

Table S4. Repeatability of stiffness measurements across three trials

	Type III Sum of Squares	Mean Square	F	*P*
Trial (2)	0.342	0.171	11.807	**0.0000**

Pairwise Comparisons

Trial		Mean Difference	S.E.	P^b
1	2	-0.073	.021	**0.0030**
	3	-0.121	.029	**0.0000**
2	1	0.073	.021	**0.0030**
	3	-0.048	.025	0.2060
3	1	0.121	.029	**0.0000**
	2	0.048	.025	0.2060

Within-subject effects from repeated-measures ANOVA of normalized, log-transformed stiffness over multiple trials.
Sample size for each group was 45.
b. Adjustment for multiple comparisons: Bonferroni.
Test of sphericity: p=0.127

Table S5. Non-normalized moments and angular deflections from Trial 1 for all specimens

Specimen 1, Trial 1

	T1-2		T3-4		T5-6		T7-8		T9-10		L1-2		L3-4		L5-S1	
	Moment (Nm)	Angle (degrees)	Moment	Angle	Moment	Angle	Moment	Angle	Moment	Angle	Moment	Angle	Moment	Angle	Moment	Angle
Dorsal extension	0.00226	1.66639	0.00361	2.70005	0.00355	1.10839	0.00359	2.32660	0.00347	1.17267	0.00340	2.05853	0.00339	1.40126	0.00438	1.45123
	0.00456	2.86788	0.00724	2.84347	0.00713	2.23450	0.00712	3.05819	0.00700	2.49443	0.00679	2.91592	0.00677	2.38866	0.00879	2.26187
	0.01133	4.59390	0.01817	5.71770	0.01781	3.89872	0.01068	4.18402	0.01045	3.31809	0.01010	3.56098	0.01015	3.15634	0.01323	2.85816
	0.01581	5.43407	0.03657	5.46593	0.03541	6.02557	0.01422	4.40080	0.01383	4.00829	0.01354	4.31850	0.01355	3.59052	0.01763	3.21180
	0.02261	6.31104	0.05422	7.53204	0.05326	6.74586	0.01777	5.05877	0.01727	4.53183	0.01684	4.82799	0.01685	4.12025	0.02203	3.70548
	0.03404	7.63390	0.07307	7.67599	0.07056	8.18528	0.02482	6.23429	0.02425	5.28076	0.02357	5.08854	0.02350	4.76556	0.03080	4.32470
	0.04559	7.41159	0.10875	8.53220	0.10519	8.52506	0.03546	6.81199	0.03473	6.29409	0.03355	5.55496	0.03350	5.69508	0.04410	4.75912
	0.07153	7.96408	0.17977	9.70380	0.17595	9.32151	0.05313	7.82271	0.05183	7.65805	0.05090	6.55108	0.05071	6.23269	0.06586	5.37496
	0.09599	7.55208	0.25094	10.79467	0.24423	10.90551	0.07098	8.39571	0.06910	8.27864	0.06740	7.26351	0.06732	6.94323	0.08714	5.79688
	0.11983	7.78504					0.10624	8.94459	0.10368	9.45485	0.10189	8.40728	0.10073	7.57846	0.13046	6.28333
	0.16974	8.05152					0.17489	10.21710	0.16935	10.35034	0.16585	9.09754	0.16730	9.64640	0.21641	7.07648
							0.24280	11.15439			0.22577	9.85460	0.23118	9.82777	0.29827	7.79656
Mediolateral flexion	0.00209	3.47330	0.00358	2.84631	0.00353	1.70473	0.00359	2.32689	0.00353	1.43586	0.00354	2.44974	0.00337	0.93610	0.00434	0.89251
	0.00413	4.44798	0.00713	4.63583	0.00704	3.40108	0.00700	3.44997	0.00707	2.68282	0.00701	3.39481	0.00672	1.91150	0.00870	1.24327
	0.01041	5.99583	0.01785	6.63282	0.01773	5.05531	0.01749	5.39323	0.01764	3.89942	0.01759	5.35855	0.01687	3.14657	0.02169	2.13989
	0.01456	7.41617	0.03541	7.70020	0.03535	7.56308	0.03484	6.28167	0.03526	5.62377	0.03507	7.21751	0.03359	4.35139	0.04334	2.82374
	0.02069	8.22180	0.05306	8.84471	0.05346	8.43792	0.05222	7.90450	0.05245	6.25367	0.05259	8.52232	0.05091	5.25171	0.06502	3.12587
	0.03105	9.66893	0.07042	9.83060	0.07021	9.64503	0.06998	8.63681	0.06958	7.43374	0.06952	8.61966	0.06757	5.48992	0.08676	3.62952
	0.04147	10.16280	0.10472	10.68785	0.10544	11.13361	0.10394	9.99544	0.10404	8.29951	0.10344	9.68189	0.10112	6.79142	0.12903	4.98370
	0.06184	12.08452	0.17313	12.11344	0.17380	12.54804	0.17557	11.79578	0.17072	9.99994	0.16992	11.62940	0.16724	8.25248	0.21409	5.93563
	0.08235	12.46242	0.23752	13.38941	0.24030	13.91557	0.24292	12.72471	0.23506	11.22594	0.22504	13.34244	0.23269	9.14093	0.29777	7.02021
	0.10204	13.07170														
	0.14037	14.17912														
Ventral flexion			0.00357	2.07409	0.00343	0.83683	0.00363	1.37184	0.00350	0.76075	0.00351	1.65604	0.00348	1.01003	0.00460	0.67027
			0.00723	3.36457	0.00683	1.49517	0.00729	2.58482	0.00702	1.54375	0.00701	2.48291	0.00698	1.52223	0.00920	1.23121
			0.01770	4.47795	0.01700	2.74455	0.01082	2.96540	0.01058	2.36896	0.01044	2.82395	0.01038	2.15905	0.01380	2.26647
			0.03529	5.56644	0.03414	3.73228	0.01443	3.59771	0.01406	2.88430	0.01396	3.77954	0.01380	3.02321	0.01840	2.31047
			0.05214	6.27060	0.05093	4.24467	0.01804	4.11619	0.01754	2.96625	0.01745	4.08330	0.01727	3.61290	0.02294	2.91604
			0.06931	6.25237	0.06743	4.83408	0.02558	4.77243	0.02461	3.69951	0.02439	5.07180	0.02418	3.96862	0.03211	3.49020
			0.10404	7.15232	0.10275	4.96272	0.03555	5.15432	0.03545	4.11628	0.03478	5.42445	0.03439	4.37102	0.04568	4.21213
			0.16979	8.16498	0.16979	5.56840	0.05367	5.98846	0.05340	5.03197	0.05223	6.22148	0.05161	5.38466	0.06800	4.68606
			0.32461	10.10386	0.23685	6.87437	0.07122	6.92216	0.06989	5.11107	0.06970	6.98542	0.06845	5.71652	0.09068	5.49320
							0.10530	7.08139	0.10493	5.82704	0.10464	7.57421	0.10251	6.25458	0.13498	5.87770
							0.17477	7.98642	0.23868	6.47276	0.17635	8.25499	0.16982	6.88163	0.22214	6.67130
							0.24101	9.21090			0.24008	8.91063	0.23377	8.09820	0.30876	6.89805

Table S5 continued: Specimen 2, Trial 1

	T1-2		T3-4		T5-6		T7-8		T9-10		L1-2		L3-4		L5-S1	
	Moment	Angle	Moment	Angle	Moment	Angle	Moment	Angle	Moment	Angle	Moment	Angle	Moment	Angle	Moment	Angle
Dorsal extension	0.00359	2.05857	0.00350	1.06274	0.00364	1.10563	0.00343	1.69811	0.00362	2.39082	0.00372	1.65480	0.00368	1.94509	0.00455	1.05978
	0.00716	3.20803	0.00703	1.84574	0.00728	1.81972	0.00684	2.58102	0.00723	3.52142	0.00740	2.84222	0.00737	2.54039	0.00915	1.55443
	0.01072	4.01979	0.01051	2.70767	0.01096	2.59105	0.01021	3.44165	0.01080	4.15155	0.01115	3.46122	0.01102	3.63127	0.01372	1.78260
	0.01434	4.01905	0.01401	3.29189	0.01455	2.89893	0.01357	3.85489	0.01441	4.48337	0.01485	3.63224	0.01467	4.04673	0.01834	2.05199
	0.01792	4.34644	0.01751	3.82240	0.01819	3.75668	0.01699	4.61265	0.01806	4.98721	0.01844	4.28175	0.01825	4.23238	0.02295	2.29331
	0.02504	4.64796	0.02440	4.15662	0.02544	4.67125	0.02375	5.24997	0.02516	5.35107	0.02587	4.75195	0.02556	5.05666	0.03209	2.87741
	0.03567	4.94775	0.03486	4.59951	0.03613	5.11391	0.03384	5.94378	0.03576	6.22957	0.03692	5.57958	0.03641	5.71041	0.04574	3.79502
	0.05333	5.54420	0.05213	5.23222	0.05404	5.84553	0.05052	6.49355	0.05356	6.53569	0.05513	6.05139	0.05414	6.31503	0.06828	4.82340
	0.07067	5.69256	0.06944	5.95221	0.07200	6.18475	0.06734	7.34560	0.07111	7.55775	0.07401	6.98641	0.07199	6.76423	0.09061	5.58238
	0.10569	6.26526	0.10386	6.21627	0.10739	6.81027	0.10134	7.98338	0.10646	7.60065	0.10997	7.60342	0.10789	6.99563	0.13557	6.30487
	0.17516	7.02412	0.17319	6.90907	0.17760	7.68096	0.16706	8.89111	0.17538	8.21994	0.18155	7.67953	0.17812	7.87964	0.22614	7.99487
	0.23946	7.60393	0.24036	7.55092	0.24347	8.29198	0.23179	9.21563	0.24205	8.87285	0.25271	8.32655	0.24599	8.58267	0.31278	9.01247
Mediolateral flexion	0.00343	3.50658	0.00340	2.82632	0.00357	2.68502	0.00375	3.62514	0.00366	3.87948	0.00379	3.38691	0.00365	2.49203	0.00435	1.54106
	0.00685	5.07696	0.00677	4.65485	0.00716	3.94383	0.00746	4.17763	0.00730	5.41927	0.00756	4.67181	0.00725	3.59785	0.00869	2.15750
	0.01358	6.93469	0.01347	5.90051	0.01427	5.03301	0.01504	5.67277	0.01454	6.80718	0.01515	5.89838	0.01446	4.48385	0.01723	2.95593
	0.01702	7.45843	0.01684	6.65416	0.01751	5.78300	0.01872	6.36872	0.01817	7.37292	0.01890	6.59771	0.01802	4.95743	0.02163	3.42980
	0.02371	7.87306	0.02348	7.38136	0.02453	6.43351	0.02620	7.19989	0.02545	8.20906	0.02636	7.35154	0.02520	5.57377	0.03028	3.89814
	0.03361	8.96683	0.03342	8.25456	0.03487	7.63336	0.03745	8.25650	0.03635	8.53640	0.03755	8.28030	0.03592	6.40846	0.04334	4.75030
	0.05003	9.45981	0.04988	9.57150	0.05196	8.01351	0.05582	9.47674	0.05404	9.99256	0.05635	9.40205	0.05363	7.60048	0.06482	5.57611
	0.06647	10.4217	0.06584	10.6764	0.06895	9.27564	0.07440	9.58219	0.07171	10.3241	0.07482	10.0165	0.07119	8.12098	0.08600	6.22489
	0.09822	11.7085	0.09791	11.6975	0.10352	10.0916	0.11112	11.0758	0.10679	11.5893	0.11123	10.9365	0.10558	9.02735	0.12783	7.40064
	0.16143	12.5065	0.16025	13.3916	0.17145	11.4856	0.18050	12.5810	0.17790	12.8340	0.18405	12.1386	0.17427	10.5625	0.20938	8.93235
	0.21796	13.9611	0.21839	15.0894	0.23545	12.7836	0.24785	14.1829	0.24625	14.2260	0.25181	13.2037	0.23990	11.6588	0.28712	10.4087
Ventral flexion	0.00356	2.14495	0.00355	1.00856	0.00360	1.28823	0.00343	2.22486	0.00369	1.84698	0.00370	1.83062	0.00362	1.75522	0.00449	1.54102
	0.00712	3.86004	0.00708	2.31025	0.00718	2.68889	0.00686	3.55872	0.00737	2.70671	0.00739	3.14085	0.00724	2.75382	0.00901	2.60756
	0.01069	4.96451	0.01060	3.05219	0.01074	3.14828	0.01026	3.99081	0.01108	3.49992	0.01106	3.52788	0.01088	3.54629	0.01343	3.42359
	0.01427	5.47250	0.01417	3.41839	0.01432	3.49812	0.01370	4.56348	0.01473	3.98979	0.01479	4.15364	0.01450	4.05175	0.01788	4.01350
	0.01789	5.99260	0.01777	3.61838	0.01789	4.01553	0.01716	4.79294	0.01841	4.61253	0.01849	4.46440	0.01808	4.84987	0.02233	4.60306
	0.02498	6.72979	0.02483	4.34992	0.02508	4.11130	0.02403	5.23429	0.02578	4.83267	0.02601	4.62271	0.02531	4.90350	0.03118	5.03913
	0.03561	7.20406	0.03554	4.87361	0.03581	4.46092	0.03422	5.27469	0.03684	5.37412	0.03717	5.09249	0.03623	5.61482	0.04449	5.55809
	0.05339	7.93740	0.05333	5.07662	0.05340	4.77222	0.05108	5.50795	0.05484	5.51789	0.05534	5.44803	0.05426	6.16659	0.06684	6.15000
	0.07103	7.98674	0.07067	5.26934	0.07119	4.93557	0.06806	6.10433	0.07337	6.39779	0.07336	6.08355	0.07204	6.46777	0.08844	6.98727
	0.10596	8.56862	0.10592	5.62782	0.10633	5.11220	0.10161	6.22446	0.10926	6.45820	0.10956	6.25671	0.10748	6.69085	0.13181	7.29688
	0.17483	8.95070	0.17452	6.27794	0.17536	5.99690	0.16827	6.82979	0.18010	7.11291	0.18262	7.21477	0.17761	7.57852	0.21877	7.87453
	0.24311	9.48859	0.24092	6.63015	0.24541	6.33839	0.23113	7.53149	0.25068	7.62508	0.25050	7.56085	0.24542	7.95555	0.30103	9.28688

Table S5 continued: Specimen 3, Trial 1

	T1-2		T3-4		T5-6		T7-8		T9-10		L1-2		L3-4		L5-S1	
	Moment	Angle	Moment	Angle	Moment	Angle	Moment	Angle	Moment	Angle	Moment	Angle	Moment	Angle	Moment	Angle
Dorsal extension	0.00372	1.15272	0.00380	0.68226	0.00376	0.76203	0.00393	1.19965	0.00386	1.24195	0.00367	0.45842	0.00394	0.78594	0.00490	0.55610
	0.00743	2.25173	0.00757	1.48959	0.00751	1.50759	0.00785	1.87052	0.00773	1.97074	0.00737	1.05978	0.00786	1.00995	0.00980	1.11484
	0.01114	3.01293	0.01134	1.94960	0.01125	2.09217	0.01178	2.46378	0.01159	2.25031	0.01105	1.44846	0.01178	1.30768	0.01470	1.50694
	0.01479	3.44689	0.01510	2.54020	0.01500	2.32542	0.01572	3.17101	0.01547	2.67170	0.01472	1.86631	0.01569	1.61531	0.01964	1.87089
	0.01851	3.91513	0.01885	2.94625	0.01878	2.74112	0.01971	3.39106	0.01934	2.93935	0.01832	1.72626	0.01959	1.84038	0.02453	2.06763
	0.02588	4.78715	0.02629	3.70469	0.02609	3.55021	0.02749	4.29784	0.02705	3.73233	0.02576	2.26793	0.02742	2.17402	0.03431	2.64473
	0.03687	5.17090	0.03751	4.61032	0.03737	4.58357	0.03933	5.22853	0.03850	4.78250	0.03662	2.85234	0.03909	2.92210	0.04880	2.87739
	0.05502	5.89923	0.05605	5.56358	0.05591	5.54453	0.05863	6.48645	0.05800	5.84621	0.05475	3.79158	0.05859	3.63764	0.07322	3.83675
	0.07357	6.17152	0.07457	6.13928	0.07443	6.30727	0.07791	7.40870	0.07706	6.69939	0.07261	4.64001	0.07807	4.91476	0.09722	4.61962
	0.10976	6.58922	0.11112	6.63916	0.11129	6.83755	0.11602	8.13748	0.11520	7.60343	0.10896	5.75628	0.11721	5.44902	0.14523	5.23692
	0.18155	7.03512	0.18350	7.54102	0.18262	7.78824	0.19254	8.92008	0.19130	8.35484	0.18091	6.82245	0.19356	6.46656	0.24008	5.94898
	0.25150	7.34936	0.25246	7.97796	0.25340	8.25899	0.26609	9.87993	0.26546	8.98189	0.25016	7.80432	0.26960	7.22857	0.33148	6.80770
Mediolateral flexion	0.00343	2.79711	0.00368	2.36601	0.00386	3.26195	0.00374	1.98234	0.00371	2.67858	0.00368	1.15851	0.00400	1.78538	0.00469	0.15363
	0.00688	3.97738	0.00736	3.38756	0.00772	4.42174	0.00750	3.32941	0.00736	3.63807	0.00732	2.42641	0.00802	2.28094	0.00934	0.67393
	0.01026	4.74534	0.01104	4.16133	0.01157	5.42850	0.01125	3.80039	0.01106	4.45128	0.01098	2.64019	0.01206	3.06465	0.01406	0.83087
	0.01370	5.53263	0.01467	4.74688	0.01547	5.72273	0.01496	4.32510	0.01465	4.74433	0.01472	3.20662	0.01608	3.78729	0.01870	1.14755
	0.01705	6.10622	0.01839	5.32878	0.01926	6.20212	0.01870	4.58736	0.01822	5.31253	0.01831	3.64897	0.02002	3.84280	0.02335	1.02533
	0.02403	6.95698	0.02565	5.73571	0.02694	6.80177	0.02616	5.29466	0.02545	5.76179	0.02563	4.21364	0.02811	4.30330	0.03280	1.49906
	0.03416	7.98191	0.03648	6.71308	0.03844	7.48620	0.03727	5.93861	0.03694	6.79865	0.03661	4.73915	0.04005	4.93348	0.04676	1.89776
	0.05150	9.10319	0.05464	7.96003	0.05776	8.41218	0.05582	6.65493	0.05527	7.52494	0.05509	5.19602	0.06008	5.81302	0.07014	2.48493
	0.06787	10.35529	0.07245	8.98608	0.07642	9.32753	0.07415	7.31927	0.07353	8.35202	0.07305	5.79130	0.07983	6.57093	0.09343	3.00026
	0.10100	11.57866	0.10814	10.11853	0.11393	10.25830	0.11051	8.31906	0.10822	9.32569	0.10895	6.59965	0.11976	7.33772	0.14003	3.77208
	0.16702	13.65610	0.17764	11.21972	0.18775	11.44143	0.18232	9.66025	0.17734	10.57762	0.18198	7.57135	0.19775	8.63471	0.23079	4.80735
	0.22966	14.83833	0.24532	12.50647	0.26027	12.31938	0.25264	10.67855	0.24740	11.83084	0.24938	8.00170	0.27618	9.49521	0.32105	6.02132
Ventral flexion	0.00365	0.99348	0.00377	1.11475	0.00375	0.92702	0.00389	1.07079	0.00394	1.30702	0.00366	0.91052	0.00399	1.56716	0.00480	1.15372
	0.00732	2.18155	0.00759	2.03475	0.00750	2.17778	0.00778	1.83220	0.00785	2.30044	0.00731	1.59848	0.00801	2.22848	0.00960	2.14708
	0.01096	2.97148	0.01136	2.65113	0.01123	3.28052	0.01170	2.51788	0.01173	3.11424	0.01101	2.42461	0.01197	3.12527	0.01433	2.66023
	0.01464	3.47061	0.01517	3.16722	0.01494	3.56245	0.01556	2.82244	0.01565	3.44592	0.01468	2.78694	0.01602	3.29765	0.01903	3.08034
	0.01830	4.14288	0.01894	3.39171	0.01862	3.99169	0.01937	2.94967	0.01961	3.93211	0.01827	3.26448	0.02002	3.92657	0.02386	3.05918
	0.02556	4.63376	0.02647	4.14415	0.02604	4.26970	0.02714	3.28947	0.02742	4.19924	0.02565	3.43180	0.02796	4.13611	0.03323	3.67789
	0.03631	5.29137	0.03784	4.27012	0.03710	4.65474	0.03861	3.71064	0.03914	4.73426	0.03665	4.09926	0.03976	4.69213	0.04742	3.86188
	0.05441	5.79678	0.05676	4.85299	0.05595	5.34420	0.05786	3.97392	0.05872	5.15474	0.05498	4.24193	0.05955	5.26796	0.07105	4.25442
	0.07267	5.96622	0.07581	5.10936	0.07415	5.43355	0.07706	4.22006	0.07770	5.28689	0.07311	4.55702	0.07974	5.53746	0.09464	4.52379
	0.10873	6.41612	0.11327	5.55261	0.11058	5.70764	0.11501	4.50216	0.11628	5.72506	0.10925	4.68063	0.11916	5.81591	0.14118	4.82241
	0.17834	6.87717	0.18764	6.08388	0.18309	6.58479	0.18982	5.03728	0.19297	6.26904	0.18122	5.27927	0.19433	6.57272	0.23327	5.30415
	0.24508	7.42059	0.26125	6.59623	0.25376	7.12426	0.26286	5.45897	0.26518	6.73696	0.25137	5.82852	0.27357	6.90423	0.32328	5.57797

Table S5 continued: Specimen 4, Trial 1

	T1-2		T3-4		T5-6		T7-8		T9-10		L1-2		L3-4		L5-S1	
	Moment	Angle	Moment	Angle	Moment	Angle	Moment	Angle	Moment	Angle	Moment	Angle	Moment	Angle	Moment	Angle
Dorsal extension	0.00355	0.85002	0.00390	0.48792	0.00423	0.75480	0.00413	2.49206	0.00422	1.19367	0.00413	0.58398	0.00410	0.47034	0.00533	0.36350
	0.00708	1.75929	0.00775	1.17305	0.00844	1.57342	0.00826	3.44596	0.00844	1.72146	0.00826	0.95010	0.00819	0.75919	0.01063	0.91105
	0.01061	1.99798	0.01163	1.96464	0.01269	1.90126	0.01239	4.08448	0.01267	2.31111	0.01236	1.48436	0.01230	1.26721	0.01595	1.13093
	0.01769	2.90671	0.01550	2.49329	0.02114	2.96158	0.02061	5.21007	0.02118	3.11641	0.02064	1.70794	0.02042	1.61722	0.02656	2.22905
	0.03165	4.48098	0.01939	2.81392	0.04221	4.33551	0.04117	6.37486	0.04229	4.77127	0.04109	3.07618	0.04077	2.67512	0.05313	2.44916
	0.03632	4.62520	0.02325	3.16557	0.08027	6.26607	0.08302	6.65927	0.08357	6.04680	0.08397	5.09295	0.07879	4.04711	0.10681	3.50406
	0.07212	6.36124	0.02711	3.47650	0.15936	7.83810	0.16352	8.45020	0.16533	7.91000	0.16495	7.00950	0.15569	5.92456	0.20899	5.05464
	0.10775	7.43228	0.03102	3.61863	0.23670	8.87943	0.24056	9.95151	0.24481	8.90537	0.24223	8.02899	0.23039	6.54382	0.30521	5.43086
	0.14266	8.27099	0.03493	4.22542	0.31152	9.57376	0.30472	10.51620	0.31959	10.00121	0.31084	9.23199	0.29956	7.50449	0.39098	6.27239
			0.07817	4.17062												
			0.15563	5.84193												
			0.23328	6.80707												
			0.30972	7.74929												
Mediolateral flexion	0.00348	2.00707	0.00384	3.21533	0.00411	3.64413	0.00349	2.97811	0.00404	2.41067	0.00417	1.85113	0.00410	1.44581	0.00509	0.63428
	0.00696	3.08417	0.00767	4.36188	0.00819	5.37024	0.00646	4.29100	0.00805	3.40262	0.00833	2.76559	0.00816	2.08235	0.01016	1.00882
	0.01044	3.82678	0.01149	5.05848	0.01229	6.08241	0.00969	4.92514	0.01207	4.31887	0.01249	3.42575	0.01223	3.00973	0.01523	1.10364
	0.01736	4.51653	0.01530	5.61325	0.02047	6.93989	0.01609	6.03559	0.02011	5.03714	0.02083	4.07097	0.02038	3.75813	0.02541	1.61084
	0.03121	5.66142	0.01912	5.95245	0.04082	8.31118	0.03205	7.30079	0.04010	6.33760	0.04165	4.85171	0.04061	4.78756	0.05083	2.19057
	0.03464	5.86703	0.02290	6.40938	0.08101	9.88172	0.06631	8.68555	0.07990	7.81434	0.08311	5.91328	0.08089	6.07883	0.10122	2.95673
	0.06898	7.11250	0.02671	6.81103	0.16009	12.07090	0.12129	10.67091	0.15843	9.49676	0.16507	7.45505	0.15960	7.61061	0.20155	4.28355
	0.10286	8.56143	0.03048	7.04368	0.23589	13.86849	0.18497	11.91107	0.23346	10.93322	0.24454	8.87719	0.23560	8.55352	0.30626	5.09891
	0.13644	9.52027	0.03426	7.37773	0.30935	14.79836	0.24955	12.94511	0.30519	11.84945	0.32031	9.72320	0.30625	9.33449	0.40047	5.83939
			0.07653	6.49717												
			0.15064	9.12977												
			0.22432	10.21435												
			0.29694	10.89908												
Ventral flexion	0.00358	0.87256	0.00408	1.41606	0.00418	1.05985	0.00418	1.42535	0.00413	1.22776	0.00417	0.85357	0.00400	0.59760	0.00549	0.64187
	0.00715	1.86025	0.00813	2.67005	0.00834	2.24037	0.00806	2.40441	0.00826	1.81006	0.00833	1.56664	0.00799	1.61850	0.01095	1.13366
	0.01074	2.32859	0.01222	3.40434	0.01254	2.94128	0.01209	3.01315	0.01243	2.47087	0.01249	2.03603	0.01199	2.01155	0.01644	1.35694
	0.01792	3.08708	0.01627	3.83671	0.02019	3.89186	0.02014	3.83899	0.02065	3.32253	0.02091	2.91369	0.01999	2.70353	0.02736	1.96116
	0.03226	4.01961	0.02031	4.45177	0.04022	5.11107	0.04008	5.12045	0.04113	4.65794	0.04167	3.69776	0.04002	3.35719	0.05476	2.87283
	0.03677	4.68346	0.02436	4.65070	0.08018	7.35575	0.07417	7.88462	0.08302	7.14748	0.08379	5.90531	0.08009	4.92353	0.10601	3.74806
	0.07345	5.68352	0.02839	4.99926	0.16445	8.46354	0.13653	8.90785	0.16459	8.18996	0.17287	6.82884	0.15975	6.00266	0.21745	4.62273
	0.11002	5.92950	0.03244	5.29879	0.24432	8.89770	0.23233	9.50335	0.24341	8.98942	0.25818	7.44534	0.23821	6.57450	0.32337	5.36456
	0.14608	6.28374	0.03648	5.54003	0.32057	9.37139	0.25415	10.45571	0.31792	9.51363	0.33995	7.99509	0.31351	7.12725	0.41811	5.62187
			0.07977	5.80653												
			0.15887	6.56564												
			0.23651	7.26810												
			0.31297	7.66016												

Table S5 continued: Specimen 5, Trial 1

	T1-2		T3-4		T5-6		T7-8		T9-10		L1-2		L3-4		L5-S1	
	Moment	Angle	Moment	Angle	Moment	Angle	Moment	Angle	Moment	Angle	Moment	Angle	Moment	Angle	Moment	Angle
Dorsal extension	0.00829	0.45363	0.00802	0.64086	0.00852	0.63554	0.00873	0.40634	0.00823	0.60502	0.00813	0.42478	0.00837	0.18707	0.01225	0.25207
	0.02071	0.99300	0.02025	0.62597	0.02125	0.96565	0.02172	1.40527	0.02059	0.79061	0.02030	1.45014	0.02091	0.76180	0.03081	0.80029
	0.04079	1.53164	0.04000	1.73650	0.04248	1.90466	0.04343	2.27662	0.04126	1.95947	0.03976	2.25844	0.04112	1.35645	0.06067	1.61132
	0.06147	2.21450	0.05915	2.16485	0.06361	2.82682	0.06499	3.27089	0.06176	2.15215	0.05961	3.06093	0.06157	1.73895	0.09096	2.02011
	0.08153	2.57179	0.08051	2.59337	0.08446	2.81723	0.08660	3.62609	0.08245	2.32431	0.08109	3.46482	0.08334	2.10291	0.12277	3.06034
	0.10169	2.98282	0.09984	3.04926	0.10589	3.37391	0.10808	4.19670	0.10277	3.30384	0.09916	4.26785	0.10428	2.67589	0.15116	3.04869
	0.12128	2.96605	0.11982	3.21709	0.12738	3.58345	0.12940	4.48235	0.12366	2.69779	0.12140	4.67339	0.12506	2.85960	0.18331	3.63627
	0.14194	3.50065	0.13893	3.64132	0.14832	3.92067	0.15045	4.73374	0.14398	4.07488	0.14215	5.10210	0.14359	3.60048	0.21118	3.86513
	0.16147	3.89792	0.15864	4.18901	0.16929	4.10480	0.17211	4.88771	0.16419	4.05024	0.16196	5.47353	0.16329	3.65353	0.24360	4.04139
	0.18209	3.84425	0.17864	4.37286	0.19036	4.48388	0.19297	5.18518	0.18391	3.88029	0.18123	6.10957	0.18416	4.22763	0.27477	4.09605
	0.20107	4.01679	0.19368	4.33921	0.21230	5.05545	0.21502	5.48262	0.20556	4.25344	0.21590	6.28946	0.20931	4.22326	0.30287	4.47752
	0.23868	3.97961	0.23842	4.41830	0.25394	5.22772	0.25624	5.57343	0.24428	4.22430	0.25812	7.16697	0.24357	4.60882	0.36250	4.66791
	0.27498	4.66308	0.27193	5.05295	0.29570	5.41004	0.29822	5.85450	0.28385	4.61511	0.30101	7.33528	0.29036	5.36627	0.42363	5.48495
	0.31427	4.87427	0.31339	5.11630	0.33805	5.96944	0.33974	6.23682	0.32342	5.11112	0.34291	7.86847	0.33157	5.53443	0.48141	5.29460
	0.34402	4.89451	0.35259	5.59192	0.37822	6.13609	0.38166	6.39003	0.36047	5.53898	0.38592	8.38534	0.36827	5.80294	0.54162	5.75669
	0.37251	5.21738	0.39104	6.18977	0.41856	6.29419	0.42303	6.71493	0.40290	5.60671	0.43107	8.73003	0.40831	6.31129	0.59982	5.99496
			0.46203	6.03335	0.50113	6.86806	0.50379	7.19999	0.46884	6.45848	0.51916	8.90594	0.49195	6.62166	0.71850	6.38838
Mediolateral flexion	0.00870	1.20560	0.00836	1.15245	0.00803	1.99083	0.00840	2.20467	0.00819	1.33203	0.00810	1.71721	0.00779	0.86299	0.01230	0.07552
	0.02173	2.42127	0.02078	2.80434	0.02015	2.80190	0.02153	3.98813	0.02058	2.69996	0.02047	4.18504	0.01956	1.70491	0.03071	0.99155
	0.04335	4.07118	0.04148	4.39120	0.04044	4.01371	0.04269	5.93126	0.04103	3.56704	0.04026	5.40109	0.03902	2.80670	0.06138	1.39744
	0.06485	4.85202	0.06238	5.09532	0.06017	4.81095	0.06428	6.22149	0.06070	4.30698	0.06051	5.96503	0.05817	3.84020	0.09215	1.27117
	0.08601	5.95675	0.08356	5.82181	0.08003	5.64952	0.08534	6.49862	0.08073	5.15772	0.08010	6.76370	0.07801	4.28328	0.12302	1.58772
	0.10713	6.58225	0.10304	6.28673	0.10032	5.82897	0.10764	7.24295	0.09979	5.61800	0.10007	6.93452	0.09737	4.71478	0.15364	1.80010
	0.12824	7.19458	0.12500	6.97505	0.12018	6.25051	0.12777	8.01437	0.12157	5.81751	0.11981	7.33659	0.11700	5.15110	0.18427	1.91941
	0.14878	7.63938	0.14502	7.45711	0.13999	6.84213	0.14868	8.27830	0.14023	6.68269	0.13945	7.94180	0.13629	5.19924	0.21466	1.59648
	0.16943	8.08796	0.16492	7.51093	0.15962	7.09142	0.16870	8.66677	0.16074	6.22094	0.15913	7.89841	0.15073	5.82808	0.24510	1.96220
	0.18940	8.37958	0.18434	8.20443	0.17959	7.67816	0.18985	8.86867	0.18150	7.18326	0.18160	8.09583	0.17487	6.27001	0.27517	1.63963
	0.20424	8.41297	0.20205	7.75879	0.20520	7.79726	0.20464	8.77134	0.20206	7.37416	0.19831	8.50508	0.20684	6.34848	0.28412	1.70990
	0.24337	9.28525	0.23918	8.11373	0.24371	8.45992	0.24638	9.78536	0.24023	8.10364	0.23783	8.68186	0.25120	6.78891	0.34084	1.93810
	0.28214	9.86901	0.27699	8.64881	0.28364	8.75005	0.28464	9.57803	0.27983	8.31936	0.27823	8.22213	0.28728	7.29685	0.39483	1.74417
	0.31875	10.55791	0.31890	9.23556	0.32401	9.12150	0.32696	10.26708	0.31701	9.15382	0.31331	8.61947	0.32769	7.76128	0.45342	1.77141
	0.35535	11.12102	0.35386	9.89345	0.36469	9.37505	0.36697	10.64059	0.35428	9.30422	0.35707	8.15895	0.36292	8.09171	0.50871	1.83363
	0.39160	11.50877	0.39528	9.98401	0.40609	9.98517	0.40638	10.96188	0.38648	9.38434	0.38951	8.57579	0.40921	8.03933	0.57575	2.00653
			0.47435	10.67896	0.48196	10.16339	0.48528	11.49989	0.45376	9.66263	0.47681	8.47943	0.47871	8.43372	0.67332	2.10871
Ventral flexion	0.00824	0.39272	0.00796	0.47510	0.02103	1.04099	0.00820	0.29855	0.00382	0.70390	0.00844	0.71591	0.00849	0.21898	0.01188	0.50522
	0.02075	0.93296	0.02003	1.20111	0.04171	1.75332	0.02066	1.29328	0.02026	1.16726	0.02109	1.26686	0.02055	0.63409	0.02943	1.40529
	0.04173	1.62517	0.03871	2.17600	0.06290	2.44832	0.04143	1.62671	0.04034	2.10276	0.04202	1.61805	0.04207	1.24010	0.05873	1.85374
	0.06266	2.32473	0.05897	2.18303	0.08379	3.07617	0.06221	2.15850	0.06042	2.28490	0.06292	2.32572	0.06118	1.90412	0.08907	2.57229
	0.08372	2.67567	0.07974	2.66597	0.10519	3.51695	0.08297	3.05759	0.08066	2.54084	0.08390	2.85017	0.08501	2.30600	0.11893	3.00560
	0.10494	3.03897	0.09848	2.64894	0.12623	3.70854	0.10291	3.47342	0.10075	2.95105	0.10538	3.07002	0.10610	2.52126	0.14648	3.25904
	0.12609	3.68958	0.12033	3.16113	0.14641	3.87880	0.12221	3.78621	0.12148	3.22048	0.12591	3.41863	0.12731	2.53407	0.17872	3.26469
	0.14730	3.84285	0.14025	3.40773	0.16776	4.00683	0.14389	3.99638	0.14126	3.37482	0.14719	3.61664	0.14745	2.67844	0.21141	3.07721
	0.16822	4.26419	0.16253	3.40650	0.18842	4.21856	0.16070	4.38384	0.16176	3.69319	0.16814	3.90478	0.16517	2.88202	0.24055	3.51936
	0.18964	4.38962	0.17711	3.42273	0.20569	4.91243	0.18686	4.43463	0.17616	3.87809	0.19080	4.05922	0.19102	3.28991	0.27013	3.57064
	0.21563	4.97786	0.20806	3.57621	0.24707	5.01837	0.20836	5.40774	0.20157	3.68742	0.20739	4.31576	0.21480	3.71838	0.30511	3.66671
	0.25658	5.59217	0.25001	3.79754	0.28662	5.33874	0.24748	5.54692	0.24277	3.27813	0.25041	4.80390	0.25741	3.99614	0.36596	4.47261
	0.30002	5.90700	0.29180	4.13774	0.32653	5.61854	0.29273	5.51009	0.28290	3.50478	0.29111	4.69003	0.29520	4.15628	0.42358	4.36230
	0.34141	6.26298	0.33361	4.15835	0.36650	5.72361	0.33235	6.06479	0.32451	3.73674	0.33369	4.94914	0.33933	4.17219	0.48415	4.97547
	0.38155	6.44171	0.37306	4.42196	0.40562	5.61318	0.37476	5.68222	0.36468	3.51136	0.37345	5.06987	0.37788	4.47955	0.54113	5.01860
	0.42176	6.69710	0.41426	4.10232	0.48812	6.08953	0.41735	6.31490	0.40473	3.67778	0.41509	5.41830	0.42121	4.58898	0.59921	4.66982
			0.49050	4.42214			0.50353	6.68224	0.48237	3.87953	0.49864	5.61942	0.49697	4.57856	0.71196	5.18356

Table S5 continued: Specimen 6, Trial 1

	T1-2		T3-4		T5-6		T7-8		T9-10		L1-2		L3-4		L5-S1	
	Moment	Angle	Moment	Angle	Moment	Angle	Moment	Angle	Moment	Angle	Moment	Angle	Moment	Angle	Moment	Angle
Dorsal extension	0.00502	0.34790	0.00487	0.26422	0.00497	0.49870	0.00518	0.29178	0.00514	0.43758	0.00513	0.18934	0.00509	0.28629	0.00632	0.24006
	0.01002	0.96795	0.00974	0.59138	0.00995	0.70827	0.01035	0.58449	0.01027	0.73764	0.01026	0.30951	0.01014	0.62248	0.01263	0.29336
	0.02504	1.96508	0.01460	0.74620	0.01490	0.89307	0.01551	0.63767	0.01543	1.11897	0.01540	0.53341	0.01520	0.73624	0.01895	0.40601
	0.04992	3.27721	0.02426	1.11387	0.02482	1.39331	0.02579	1.25367	0.02566	1.77422	0.02566	0.99230	0.02528	1.08936	0.03150	0.71409
	0.09952	4.49104	0.03393	1.60019	0.03479	1.78724	0.03623	1.74302	0.03583	2.47456	0.03582	1.57880	0.03554	1.69855	0.04411	1.20666
	0.14801	4.86888	0.04854	2.18729	0.04970	2.22517	0.05170	2.62473	0.05125	2.98373	0.05117	2.03533	0.05056	2.47759	0.06304	1.68076
	0.24493	5.80504	0.09673	3.13709	0.09934	3.41023	0.10255	4.33069	0.10101	4.88385	0.10361	4.21873	0.10293	3.07151	0.13043	2.59582
	0.33976	6.45910	0.14452	3.75183	0.14827	4.47577	0.15278	5.08065	0.15061	5.89879	0.15453	5.23356	0.15343	4.37679	0.19443	3.50461
	0.47644	7.21717	0.23890	4.71378	0.24607	5.07624	0.25188	6.23894	0.24790	7.34322	0.25548	6.37720	0.25208	5.60734	0.32079	4.38831
			0.33224	5.53486	0.34130	5.91989	0.34796	6.91220	0.34168	8.15711	0.35297	7.44706	0.34845	6.45682	0.44293	5.25908
			0.46616	5.91125	0.47903	6.57038	0.47910	7.93349	0.47399	8.78978	0.49333	8.20514	0.48694	7.26268	0.61823	5.73070
Mediolateral flexion	0.00497	1.10350	0.00484	0.72132	0.00517	1.17210	0.00495	1.49757	0.00510	1.32649	0.00510	0.91923	0.00502	1.08693	0.00629	0.27666
	0.00995	2.11388	0.00964	1.55872	0.01034	2.06135	0.00989	2.32191	0.01019	2.14359	0.01019	1.64410	0.01002	1.56641	0.01259	0.34922
	0.02483	3.55763	0.01444	2.15900	0.01552	2.84616	0.01483	3.09448	0.01530	2.94135	0.01530	2.17765	0.01502	1.92506	0.01891	0.61981
	0.04959	5.02749	0.02403	3.16935	0.02579	3.71741	0.02464	4.08412	0.02547	3.54231	0.02547	2.87300	0.02506	2.38033	0.03152	0.81516
	0.09867	6.74273	0.03357	3.75764	0.03618	4.08283	0.03448	4.85733	0.03561	4.25145	0.03561	3.30785	0.03498	2.87951	0.04411	0.91692
	0.14786	8.02284	0.04767	4.56978	0.05152	4.90272	0.04902	5.55595	0.05086	4.83803	0.05086	3.90136	0.04995	3.29188	0.06309	1.09996
	0.24420	9.00269	0.09445	5.74771	0.10273	6.35810	0.09725	6.84417	0.10123	6.17395	0.10123	5.05976	0.09953	4.36703	0.12608	1.62216
	0.33880	9.99350	0.14054	6.76245	0.15362	7.32165	0.14475	7.82714	0.15167	6.86273	0.15167	5.81828	0.14898	4.91884	0.18899	2.09935
	0.47810	10.85094	0.23094	7.87157	0.25350	8.73913	0.23796	8.85644	0.25051	7.93555	0.25051	6.44928	0.24525	6.07683	0.31352	2.66078
	2.00000	1.00000	0.31781	8.86941	0.35074	9.84596	0.32696	9.83868	0.34729	8.65342	0.34729	6.99136	0.33970	6.55075	0.43746	3.19169
	2.00000	1.00000	0.44367	9.67424	0.49267	10.64538	0.45312	10.65362	0.48589	9.34110	0.48589	7.56521	0.47297	7.38405	0.61929	3.69536
Ventral flexion	0.00490	0.10079	0.00497	0.32890	0.00504	0.16706	0.00498	0.28647	0.00504	0.11758	0.00523	0.20939	0.00501	0.55494	0.00648	0.33312
	0.00980	0.50576	0.00993	0.68281	0.01007	0.65910	0.00994	0.73332	0.01010	0.71865	0.01045	0.42951	0.01004	0.59208	0.01297	0.47238
	0.02451	1.55344	0.01489	0.83233	0.01510	1.06557	0.01497	1.20467	0.01513	0.97082	0.01569	0.60735	0.01504	0.77047	0.01946	0.74468
	0.04900	2.25136	0.02488	1.52284	0.02522	1.57762	0.02498	1.69159	0.02525	1.53037	0.02615	1.18729	0.02513	1.30716	0.03245	1.18821
	0.09812	3.55997	0.03478	1.98196	0.03525	2.03526	0.03501	1.96754	0.03528	1.86604	0.03664	1.51157	0.03518	1.56373	0.04551	1.35356
	0.14689	4.85846	0.04979	2.71830	0.05024	3.63720	0.04992	2.78822	0.05043	2.26136	0.05241	1.81846	0.05032	1.92211	0.06497	1.62753
	0.24487	5.63343	0.09856	4.14650	0.10058	4.30332	0.10022	3.88369	0.09922	3.41836	0.10396	2.98550	0.10106	3.28941	0.13432	2.37819
	0.34019	6.26454	0.14768	4.60828	0.15051	4.59507	0.15063	4.36597	0.14895	3.85944	0.15587	3.51131	0.15213	3.75039	0.20161	2.81616
	0.48204	6.51881	0.24613	5.12712	0.24958	5.15594	0.25048	5.03604	0.24808	4.61072	0.25949	3.99843	0.25294	4.38161	0.33540	3.17815
			0.34328	5.48800	0.34760	5.52798	0.34848	5.36312	0.34586	4.81419	0.36210	4.39452	0.35307	4.77248	0.46872	3.46469
			0.48693	6.09761	0.48949	5.88992	0.49190	5.90558	0.48988	5.10931	0.51139	4.75599	0.49973	5.03608	0.66607	3.89135

Table S5 continued: Specimen 7, Trial 1

	T4-5		T7-8		T9-10		L1-2		L3-4		L5-S1	
	Moment	Angle	Moment	Angle	Moment	Angle	Moment	Angle	Moment	Angle	Moment	Angle
Dorsal extension	0.02256	0.26922	0.02293	0.34726	0.02247	0.29686	0.02170		0.01984	0.06634	0.03040	0.64761
	0.04512	0.27833	0.04580	0.37750	0.04494	0.71200	0.04334	0.21582	0.03967	0.72669	0.06082	0.86882
	0.06768	0.43743	0.06871	0.83343	0.06748	1.09419	0.06501	0.86503	0.05959	0.99233	0.09122	1.14842
	0.09062	0.51197	0.09149	0.81007	0.08998	1.19351	0.08669	1.04972	0.07937	1.16874	0.12178	1.38410
	0.11314	0.80891	0.11467	1.40935	0.11253	1.65427	0.10828	1.37388	0.09911	1.49107	0.15207	1.63916
	0.13617	1.00195	0.13742	1.27733	0.13517	1.87460	0.12975	1.63460	0.11882	1.47640	0.18230	2.31710
	0.15887	0.83899	0.16033	1.65080	0.15791	2.03694	0.15124	1.97959	0.13869	1.86487	0.21290	2.51572
	0.18134	1.42441	0.18324	1.61136	0.18057	2.04827	0.17300	2.25036	0.15884	1.85904	0.24331	2.75497
	0.20401	1.76845	0.20615	1.71254	0.20302	2.18573	0.19447	2.39508	0.17851	2.64403	0.27411	2.80803
	0.24184	3.04541	0.23187	3.48796	0.22128	2.47999	0.21157	3.01153	0.20169	2.49744	0.30579	1.84286
	0.28937	3.22581	0.27714	3.29710	0.26569	2.90211	0.25330	3.63881	0.24253	2.84748	0.36651	2.17263
	0.33420	3.60677	0.32472	3.49520	0.31032	3.25105	0.29552	3.57141	0.28302	2.99288	0.42808	2.76392
	0.38548	3.63050	0.36966	3.49842	0.35493	3.49476	0.33735	3.71458	0.32309	3.46960	0.48926	2.46771
	0.43621	4.44460	0.41653	4.08680	0.39938	4.00535	0.37988	4.20088	0.36275	4.03193	0.55109	3.67413
	0.48353	4.10904	0.46162	3.46841	0.44376	3.85650	0.42161	4.51678	0.40340	4.28278	0.61367	3.45829
	0.72509	4.99861	0.68730	5.55274	0.66632	4.77151	0.62993	5.21077	0.60368	4.89887	0.91113	4.09722
Mediolateral flexion	0.02071	1.18393	0.02101	1.00543	0.02141	1.46591	0.02144	1.28586	0.02130	1.98069	0.03123	0.63545
	0.04171	2.27045	0.04224	1.88238	0.04287	2.29016	0.04286	2.68058	0.04258	3.18879	0.06240	1.02573
	0.06221	2.53114	0.06326	2.56547	0.06426	2.98791	0.06430	3.58492	0.06374	3.35440	0.09340	1.17841
	0.08301	3.24147	0.08437	2.89812	0.08577	3.57616	0.08573	4.00579	0.08492	3.54463	0.12444	1.54684
	0.10403	3.42440	0.10572	3.14565	0.10713	3.92531	0.10705	4.24010	0.10597	3.61366	0.15553	1.96991
	0.12443	3.94974	0.12628	3.60613	0.12867	4.16682	0.12861	4.65046	0.12693	3.98478	0.18663	1.80136
	0.14570	4.27418	0.14745	3.94832	0.14994	4.56735	0.15004	4.96370	0.14808	4.08132	0.21776	2.02020
	0.16682	4.48584	0.16876	4.10694	0.17124	4.90735	0.17143	5.44618	0.16917	4.08624	0.24859	2.05317
	0.18773	4.80911	0.18987	4.45171	0.19290	4.94919	0.19274	5.19533	0.19013	4.25160	0.27935	2.24967
	0.22031	5.23275	0.20501	4.60326	0.20992	4.88656	0.21330	5.58590	0.20781	5.27392	0.29820	3.15110
	0.26419	5.51546	0.24682	5.08680	0.25215	5.40999	0.25597	5.74460	0.24918	5.48849	0.35782	2.35664
	0.30868	6.20888	0.28745	5.29946	0.29421	5.64595	0.29811	6.18649	0.29081	5.68626	0.41758	3.24815
	0.35688	6.60371	0.32874	5.44902	0.33626	5.73040	0.34031	6.31705	0.33103	5.97042	0.47659	2.68880
	0.39387	6.92573	0.36955	5.97661	0.37729	5.95018	0.38285	6.75226	0.37244	5.55520	0.53635	3.86689
	0.43781	7.27146	0.41176	5.98390	0.41889	6.22915	0.42464	6.95742	0.41271	5.55520	0.59336	3.72420
	0.66277	8.37358	0.61703	6.81869	0.62598	7.04991	0.63510	7.88868	0.61382	5.36792	0.88829	3.72530
Ventral flexion	0.02101	0.48855	0.02212	0.54600	0.02187	0.36508	0.02166	0.20781	0.02148	0.72203	0.03132	0.93595
	0.04199	1.13379	0.04469	0.99198	0.04369	0.80864	0.04334	0.80540	0.04287	1.29148	0.06264	2.06501
	0.06296	1.47436	0.06732	1.21240	0.06549	1.72410	0.06405	1.08200	0.06425	1.71154	0.09395	2.49938
	0.08406	2.04395	0.08949	1.89218	0.08726	2.04339	0.08538	1.68022	0.08577	2.12426	0.12528	2.75811
	0.10535	2.33045	0.11646	2.32491	0.10896	2.51072	0.10686	2.05812	0.10722	2.51512	0.15641	2.81494
	0.12664	2.84175	0.13975	2.67414	0.13059	2.83782	0.12812	2.14622	0.12882	2.97082	0.18771	3.05624
	0.14777	3.05460	0.16308	3.07312	0.15237	2.99157	0.14962	2.50480	0.15025	2.99099	0.21893	3.34324
	0.16901	3.10678	0.18245	3.26438	0.17400	3.31131	0.17099	2.57190	0.17177	3.20875	0.24995	3.46931
	0.18979	3.36187	0.20494	3.38646	0.19552	3.45616	0.19232	2.76850	0.19345	3.50433	0.28090	3.50835
	0.21702	2.40809	0.21470	3.30976	0.20731	4.28697	0.22075	3.23057	0.22520	3.82109	0.32211	3.97668
	0.26201	2.99202	0.25686	3.47713	0.24867	4.77287	0.26541	3.29269	0.27032	4.58019	0.38611	4.62497
	0.30529	2.90009	0.29903	3.68280	0.28909	4.55944	0.30995	4.18970	0.31566	5.16172	0.45055	4.01516
	0.34700	3.23487	0.34245	3.06490	0.33124	4.75742	0.35367	4.19468	0.36132	4.64422	0.51143	3.14920
	0.38997	3.29327	0.38772	3.91104	0.37103	4.35487	0.39962	4.63076	0.40780	4.64422	0.57404	3.69314
	0.43575	3.34949	0.42571	3.99670	0.41259	5.00539	0.44171	5.16760	0.45219	5.04784	0.63718	4.60547
	0.64600	3.56811	0.63978	4.25407	0.61591	5.45775	0.66655	5.23923	0.67737	5.11122	0.95172	4.35218

Table S5 continued: Specimen 8, Trial 1

	T1-2		T3-4		T5-6		T7-8		T9-10		L1-2		L3-4		L5-S1	
	Moment	Angle	Moment	Angle	Moment	Angle	Moment	Angle	Moment	Angle	Moment	Angle	Moment	Angle	Moment	Angle
Dorsal extension	0.00957	0.13760	0.00929	0.07765	0.00953	0.20450	0.01067	0.48691	0.01117	0.02172	0.01079	0.14082	0.01145	0.31078	0.01481	0.14999
	0.02372	0.25760	0.02317	0.07158	0.02386	0.05247	0.02696	0.49776	0.02795	0.38475	0.02694	0.43901	0.02860	0.31279	0.03741	0.26996
	0.03328	0.54908	0.03236	0.30219	0.03340	0.19013	0.03776	0.85989	0.03908	0.56298	0.03761	0.29618	0.04002	0.63695	0.05169	0.49260
	0.04687	0.53242	0.04634	0.14477	0.04772	0.21084	0.05162	0.93462	0.05559	0.79109	0.05346	0.75534	0.05710	0.83296	0.07402	0.67794
	0.05617	0.70549	0.05575		0.05708	0.17527	0.06357	0.96506	0.06666	0.93117	0.06430	0.89441	0.06850	0.98810	0.08850	0.82000
	0.07007	0.76492	0.06960	0.44163	0.07141	0.45783	0.07931	1.30548	0.08342	1.05269	0.08022	1.18302	0.08563	1.15085	0.11199	1.34885
	0.07942	0.94282	0.07889	0.21087	0.08086	0.48262	0.08996	1.20178	0.09454	1.30053	0.09046	0.91025	0.09693	1.32714	0.12562	1.31319
	0.09337	0.78623	0.09281		0.09497	0.63235	0.10564	1.48981	0.11122	1.31417	0.10647	1.49953	0.11392	1.67048	0.14761	1.47562
	0.11648	1.18626	0.11602	0.47013	0.11863	0.85789	0.13159	1.76406	0.13909	1.54273	0.13281	1.65674	0.14216	2.02417	0.18411	1.77202
	0.14168	1.45086	0.13940	0.25259	0.14187	0.70942	0.15677	1.77216	0.16670	1.72821	0.15913	1.94830	0.17039	2.17715	0.22002	2.11234
	0.18787	3.15115	0.18576	0.94685	0.18469	1.50326	0.21146	2.14647	0.21773	2.03811	0.20128	2.32396	0.22798	3.71205	0.29119	2.11775
	0.27836	4.03436	0.27331	1.55883	0.27382	1.90665	0.31607	2.85754	0.32634	3.21044	0.29935	2.74531	0.34039	4.67777	0.43340	2.60934
	0.36859	6.31726	0.36418	1.81192	0.36219	2.16043	0.41806	2.90449	0.43145	3.36996	0.39345	3.56123	0.44953	5.47892	0.57237	3.10749
	0.45334	3.46253	0.45299	2.23305	0.44905	2.37920	0.52876	3.60056	0.53502	3.67219	0.48548	3.85346	0.55635	5.89085	0.70084	3.83252
Mediolateral flexion	0.00885	0.50563	0.00750	0.65837	0.00885	0.69003	0.01169	0.71463	0.01131	0.85680	0.01170	1.24584	0.01175	0.81404	0.01490	0.22707
	0.02220	1.41909	0.01898	0.99139	0.02219	1.35638	0.02928	2.59118	0.02843	2.18880	0.02953	2.32720	0.02928	1.85009	0.03725	0.11784
	0.03104	2.21703	0.02680	0.99146	0.03103	2.35778	0.04092	3.27965	0.03977	2.79336	0.04133	2.95471	0.04100	2.61899	0.05215	0.20400
	0.04375	3.38592	0.03840	2.64637	0.04393	2.85856	0.05817	4.91904	0.05644	3.29738	0.05866	3.56986	0.05853	3.45151	0.07448	0.52779
	0.05326	3.96651	0.04602	3.30387	0.05276	3.48307	0.06995	5.18627	0.06768	4.27067	0.06789	4.53018	0.07007	3.61297	0.08937	0.30836
	0.06647	4.59873	0.05753	3.96519	0.06570	4.25483	0.08744	5.96006	0.08477	4.53759	0.08826	4.49003	0.08748	4.19359	0.11172	0.22746
	0.07499	5.11840	0.06521	3.65336	0.07446	4.35391	0.09938	6.46043	0.09594	4.70617	0.10009	4.95050	0.09926	4.61437	0.12661	0.49328
	0.08721	5.65537	0.07718	4.97442	0.08719	5.09422	0.11604	6.96920	0.11309	5.05896	0.11828	5.26110	0.11670	4.75663	0.14906	0.59862
	0.11002	6.44966	0.09648	5.30836	0.10857	5.35653	0.14524	7.64550	0.14118	5.87384	0.14764	5.57409	0.14564	5.04162	0.18618	0.91150
	0.13181	6.84369	0.11515	6.24692	0.13014	6.08494	0.17405	8.43709	0.16908	6.25501	0.17772	6.01817	0.17430	5.13286	0.22326	1.33299
	0.17385	7.87053	0.15513	6.98131	0.17232	7.01897	0.23112	8.51730	0.22485	6.94120	0.23643	6.30351	0.23173	5.68800	0.31287	2.05724
	0.26038	8.88558	0.23118	7.34499	0.25543	7.80107	0.34413	9.79869	0.33527	7.46900	0.35399	7.37762	0.34731	6.77665	0.46792	3.83367
	0.34608	9.68930	0.31373	8.47164	0.33779	8.28917	0.45212	10.24447	0.44643	8.14459	0.46928	7.90734	0.46131	7.23677	0.62141	2.59796
	0.43245	10.13308	0.38354	8.51515	0.41630	8.50587	0.56280	10.83676	0.55619	8.86404	0.58737	8.39326	0.57098	7.58763	0.77374	3.36196
Ventral flexion	0.00877	0.28043	0.00893	0.12747	0.02288	0.63408	0.01156	0.27947	0.01155	0.20942	0.01062	0.50403	0.01112	0.29481	0.01535	0.34996
	0.02193	0.46625	0.02236	0.28664	0.03246	0.62665	0.02897	0.47574	0.02891	0.53707	0.02584	0.64367	0.02776	0.70912	0.03841	1.03069
	0.03073	0.36628	0.03118	0.30660	0.04695	0.94511	0.04058	0.79943	0.04048	0.84508	0.03716	1.27939	0.03889	1.11031	0.05378	1.45046
	0.04391	0.62211	0.05191	0.58161	0.05582	0.89396	0.05812	1.34646	0.05784	1.38817	0.05273	1.78639	0.05480	1.94391	0.07686	1.90345
	0.05278	1.20301	0.06469	0.66225	0.06809	1.42036	0.06983	1.57579	0.06929	1.93369	0.06223	2.17404	0.06587	2.11910	0.09227	1.96144
	0.06617	1.55904	0.07356	0.80678	0.07902	1.49492	0.08741	2.47441	0.08682	2.24683	0.07790	2.43801	0.08345	2.50316	0.11535	2.54345
	0.07515	1.72946	0.08654	0.97327	0.09360	1.80340	0.09933	2.82336	0.09807	2.66159	0.08819	2.94556	0.09442	2.77575	0.13063	2.70333
	0.08844	2.06117	0.10777	1.53284	0.11796	2.53850	0.11702	3.17236	0.11553	3.07983	0.10372	3.20174	0.11116	3.06428	0.15416	3.18731
	0.11076	2.94738	0.12987	2.00094	0.13948	2.79262	0.14649	3.93215	0.14426	3.39057	0.13285	3.61340	0.13920	3.32200	0.19218	3.79930
	0.13629	3.96615	0.18491	2.58165	0.18104	2.89054	0.17609	4.29037	0.17327	3.91721	0.15645	4.02434	0.16742	3.47095	0.23102	3.53483
	0.17263	4.60894	0.27497	3.36420	0.27487	3.92875	0.23444	5.35674	0.22713	4.59852	0.21087	4.45851	0.21902	4.33695	0.29735	3.73934
	0.25826	5.63571	0.36344	3.64858	0.36700	4.59716	0.34767	6.57961	0.33944	5.35637	0.32537	4.66446	0.32780	4.82273	0.44541	3.94047
	0.34651	5.81657	0.45109	4.12849	0.45442	5.22133	0.46148	6.77907	0.45147	5.76026	0.43279	5.09373	0.43636	5.03705	0.59042	4.65964
	0.42942	6.00351					0.57341	7.38211	0.56065	5.98084	0.54161	5.61382	0.55290	5.21553	0.74406	4.71520

Non-normalized moments and resulting deflection angles for all specimens in trial 1 (see Methods for calculations and explanation of missing values). Moments are in Newton metres and angles are in degrees.

Table S6. Non-normalized morphometric measurements for all specimens

		PZA	NSA	TPAD	TPAC	NSL	CL	NSH	CW	CH	PZW	IZD	TPW	TPLT	LW
Specimen 1	T1	116.8	137.2	184.9	100.9	4.5	7.0	8.2	10.3	5.4	11.4	11.3	20.9	3.0	7.2
	T2	115.1	118.9	202.0	95.6	4.7	7.8	7.5	8.0	5.3	11.9	12.2	22.4	2.6	7.7
	T3	109.7	114.4	210.8	98.1	5.3	8.4	7.6	7.7	5.4	12.1	12.1	23.7	4.7	7.7
	T4	109.8	116.3	209.8	96.0	5.3	8.0	7.1	7.7	4.8	12.1	12.1	24.4	4.9	7.8
	T5	111.7	122.3	204.1	93.3	5.4	8.2	7.4	7.5	5.0	12.2	12.4	26.2	5.2	7.8
	T6	107.4	130.3	187.9	96.7	5.3	8.2	7.0	7.7	5.3	12.2	12.4	27.5	4.9	7.6
	T7	109.4	141.0	189.7	94.6	5.6	8.6	6.9	7.7	5.4	12.2	12.5	28.6	5.1	8.0
	T8	115.3	153.6	186.7	91.3	5.6	9.0	7.0	7.4	5.3	12.6	12.3	29.9	4.9	8.0
	T9	124.8	167.9	174.0	94.5	5.6	8.1	6.7	7.8	5.3	12.8	12.5	30.5	4.5	8.4
	T10	138.8	165.4	166.9	101.5	6.2	9.2	7.0	8.1	5.2	13.1	13.0	30.5	4.0	7.4
	L1	120.8	169.7	163.0	95.6	5.9	9.0	7.1	8.0	5.4	12.5	13.3	28.1	4.6	7.7
	L2	121.7	170.4	171.3	94.7	5.8	9.0	6.9	7.8	5.4	12.8	13.2	27.5	4.5	7.9
	L3	120.6	176.2	174.9	97.2	6.0	8.7	6.8	8.0	5.5	13.1	13.1	26.3	4.1	8.2
	L4	123.2	182.9	197.3	89.9	5.8	8.4	6.7	8.2	5.2	13.3	12.6	25.6	3.6	8.3
	L5	125.3	189.0	205.0	91.2	5.6	8.5	6.9	8.1	5.4	13.1	12.8	22.7	2.8	8.4
	S1	127.0	210.2	188.6	84.8	6.2	8.8	7.1	10.6	5.1	12.4	12.1	32.6	7.3	8.1
Specimen 2	T1	109.6	158.2	190.4	114.8	3.9	7.3	10.2	10.5	5.5	10.7	11.4	20.1	2.7	6.9
	T2	125.0	143.9	194.9	113.1	4.1	7.3	9.7	10.3	5.1	11.0	11.6	20.9	2.6	7.3
	T3	131.6	134.9	201.3	107.8	4.3	7.8	9.6	8.0	5.3	11.9	11.7	23.1	2.7	7.6
	T4	125.7	137.4	203.9	103.4	5.2	7.9	8.6	7.7	5.0	12.2	11.7	25.6	4.3	7.8
	T5	124.9	140.5	201.2	108.5	5.0	7.8	8.2	7.7	4.9	12.1	12.0	26.4	4.7	7.8
	T6	117.3	149.4	193.9	97.4	5.5	8.2	8.2	7.5	5.1	12.2	11.7	27.7	4.7	7.8
	T7	136.7	154.5	193.7	100.5	5.8	8.6	8.4	7.8	5.2	12.7	12.2	29.9	4.3	7.7
	T8	127.5	166.4	180.0	97.6	5.8	8.5	8.6	7.6	5.2	12.6	12.3	29.9	4.6	7.7
	T9	134.4	165.7	176.4	98.1	6.4	8.6	8.4	8.0	5.5	12.8	12.2	30.5	4.6	7.7
	T10	138.9	178.8	174.8	98.5	6.4	8.4	8.0	8.1	5.5	12.6	13.0	30.3	4.0	7.6
	L1	128.6	179.3	174.6	100.0	6.3	8.7	7.8	8.1	5.4	12.6	12.7	30.4	3.7	7.6
	L2	120.8	187.0	170.2	95.6	6.2	8.8	8.1	7.9	5.2	12.8	12.8	28.5	3.4	7.9
	L3	123.6	185.9	180.8	93.8	5.7	8.9	8.0	7.4	5.7	13.5	13.5	25.3	3.3	8.2
	L4	133.8	180.8	185.3	93.7	5.7	8.5	7.9	8.5	5.5	14.0	13.1	24.6	2.9	8.2
	L5	127.6	189.0	191.8	93.2	5.6	8.1	8.1	8.7	5.4	13.6	12.7	23.7	2.3	8.2
	S1	129.0	207.6	210.4	84.8	5.7	8.6	7.6	9.4	5.3	13.2	11.8	31.4	5.3	7.9
Specimen 3	T1	108.4	161.6	192.4	109.8	5.1	8.0	10.8	12.1	6.2	12.8	12.8	23.8	3.0	8.5
	T2	117.4	142.1	196.3	98.9	6.0	8.5	10.1	12.1	6.4	13.4	13.5	25.0	3.3	8.5
	T3	113.4	129.0	214.5	100.6	6.3	9.0	9.6	9.2	6.4	14.2	13.5	28.1	5.2	8.9
	T4	105.5	123.7	203.6	95.0	6.6	9.1	9.2	9.2	6.1	14.3	13.9	29.3	5.2	8.9
	T5	107.2	131.1	199.8	94.6	7.1	9.3	9.1	9.0	5.9	14.1	13.5	32.4	5.6	8.4
	T6	113.3	129.9	189.3	95.1	6.8	9.1	9.1	9.1	5.9	14.3	13.9	31.4	5.4	8.6
	T7	108.8	132.7	196.8	96.5	6.7	9.0	8.7	9.1	6.1	13.9	14.4	32.8	5.8	8.6
	T8	101.0	142.0	188.4	97.1	7.2	9.9	8.2	9.0	6.0	13.8	14.2	35.8	5.6	8.7
	T9	121.3	156.6	167.9	101.1	7.3	9.9	8.3	9.3	6.0	14.5	14.5	35.1	5.4	8.5
	T10	119.9	168.6	166.2	95.5	7.5	9.4	8.3	9.4	6.1	14.6	14.1	35.9	4.9	8.8
	L1	125.7	178.3	167.2	99.8	7.2	9.2	8.4	9.7	6.0	14.9	14.0	35.5	5.0	9.1
	L2	117.8	172.5	167.6	97.9	7.8	10.0	8.3	9.9	6.2	14.9	14.8	33.6	4.5	9.1
	L3	129.3	178.0	168.5	96.6	7.7	10.2	8.7	9.8	6.3	15.4	14.8	31.5	4.2	9.4
	L4	127.4	168.9	171.2	92.2	7.3	9.7	8.6	10.0	6.4	15.9	14.5	30.5	3.6	9.6
	L5	130.6	181.6	200.0	93.3	6.5	8.7	8.3	9.9	6.4	16.3	14.3	29.0	3.2	9.8
	S1	125.8	200.4	199.0	89.3	6.7	10.1	8.6	11.4	6.2	15.4	13.5	38.3	7.1	8.7

Table S2 continued

		PZA	NSA	TPAD	TPAC	NSL	CL	NSH	CW	CH	PZW	IZD	TPW	TPLT	LW
Specimen 4	T1	89.4	109.4	147.9	193.4	5.9	10.5	13.9	13.5	7.1	12.3	13.8	27.0	4.4	8.6
	T2	105.9	104.6	134.8	204.9	6.6	10.8	13.3	13.7	7.2	13.3	15.2	29.1	5.1	9.3
	T3	105.8	108.7	129.8	205.1	7.2	11.3	12.2	11.1	7.4	14.6	15.6	31.9	6.5	9.5
	T4	100.4	102.5	138.5	205.2	7.7	11.5	11.2	10.4	7.3	14.9	15.6	36.0	7.1	9.4
	T5	107.4	94.8	139.0	202.4	7.8	11.6	10.7	10.4	6.9	14.6	16.0	38.6	6.9	9.3
	T6	101.7	97.1	145.2	197.5	7.9	11.6	10.7	10.3	7.0	14.6	15.9	40.7	7.1	9.7
	T7	105.8	99.8	143.9	192.9	7.9	12.2	10.3	10.4	7.1	14.7	16.2	41.2	6.9	9.7
	T8	108.2	96.0	156.9	179.4	7.6	11.8	10.2	10.5	7.2	14.9	16.5	43.2	6.9	9.9
	T9	112.1	96.5	164.0	178.2	7.9	12.0	9.7	10.7	7.2	15.1	16.4	44.1	6.5	9.9
	T10	114.0	95.9	174.6	173.8	8.6	12.0	10.7	10.8	7.3	15.4	16.3	43.9	6.5	10.0
	L1	124.0	91.0	185.7	170.2	7.9	12.3	10.2	11.2	7.3	15.8	16.8	42.4	6.1	9.8
	L2	120.1	90.9	197.6	172.0	8.2	12.5	10.1	11.2	7.7	15.8	17.5	38.7	5.9	9.9
	L3	119.5	93.5	190.4	172.3	8.6	12.5	10.2	11.2	7.9	16.1	17.4	37.3	5.4	10.2
	L4	124.1	89.4	182.9	182.0	8.2	12.2	10.0	11.4	7.9	17.3	17.2	35.8	4.5	10.8
	L5	123.4	82.2	189.1	184.9	7.6	11.9	10.1	11.9	7.8	17.0	16.4	33.4	3.9	10.9
	S1	115.3	86.6	213.1	201.7	8.3	12.0	9.2	12.6	7.7	16.3	16.3	43.3	8.2	9.2
Specimen 5	T1	95.9	99.0	148.1	190.7	7.5	12.7	20.4	18.4	9.6	16.7	18.6	35.6	4.6	11.1
	T2	105.4	101.0	131.2	194.1	8.0	13.3	19.2	19.1	9.4	17.8	19.7	36.0	5.8	11.5
	T3	99.9	99.0	122.0	199.5	8.7	14.4	18.3	14.3	9.7	18.8	19.4	40.7	6.8	11.8
	T4	96.3	101.0	133.0	207.1	9.3	14.2	17.8	13.3	9.0	19.1	20.2	44.6	8.0	11.6
	T5	102.8	94.0	138.2	200.8	8.8	14.0	17.2	13.4	8.7	19.2	19.9	47.6	7.1	11.6
	T6	103.0	94.0	140.0	195.2	9.0	14.8	17.0	13.1	8.7	19.5	20.1	50.1	7.6	11.5
	T7	106.9	90.0	159.1	193.5	9.2	15.1	16.4	13.1	8.9	19.6	21.0	52.1	7.6	11.5
	T8	108.9	91.0	163.5	186.1	8.9	14.8	16.0	12.8	9.1	19.4	18.8	53.9	6.5	10.2
	T9					8.7	14.1	16.6	13.5	9.3	20.0	21.2	47.9	7.3	11.6
	T10	124.0	89.0	170.4	176.7	9.5	14.6	16.2	13.6	9.0	20.4	20.2	56.0	6.9	11.9
	L1	132.5	88.0	189.1	178.8	9.9	15.6	15.9	13.9	9.6	21.1	21.8	55.7	7.3	12.2
	L2	126.3	88.0	191.8	186.7	9.7	15.8	16.0	13.7	10.1	21.6	21.8	51.8	7.2	12.2
	L3	124.9	87.0	188.7	185.7	10.0	15.4	16.1	14.1	10.6	21.9	22.7	48.7	5.9	12.1
	L4	120.5	88.0	182.3	195.2	9.4	14.9	16.0	14.6	10.3	22.7	21.5	46.5	5.5	12.0
	L5	112.3	82.0	189.2	202.1	8.4	14.3	16.1	14.9	9.9	21.7	21.4	42.9	4.9	12.0
	S1	100.2	84.0	209.5	206.5	8.5	15.1	15.5	16.3	9.6	20.1	19.6	56.0	11.0	11.0
Specimen 6	T1	107.3	110.9	130.4	191.4	6.7	12.1	16.9	16.5	8.3	14.3	17.6	31.2	4.2	10.3
	T2	114.5	111.0	124.9	203.0	7.6	12.1	16.7	16.4	8.2	15.4	18.5	34.8	4.5	11.0
	T3	113.2	109.9	131.9	198.9	8.3	13.0	15.3	12.5	8.3	16.8	18.3	39.8	8.1	11.5
	T4	106.1	104.2	135.8	202.9	8.8	13.1	14.5	12.2	7.7	18.1	18.5	43.3	7.8	11.2
	T5	108.4	102.5	146.8	196.7	8.7	13.2	13.8	11.8	8.0	17.0	18.5	47.0	7.6	11.1
	T6	105.6	101.9	148.4	192.9	9.3	13.5	13.8	11.6	8.2	16.7	19.2	48.1	7.8	11.0
	T7	112.2	100.8	151.3	183.9	9.3	13.6	13.2	11.7	8.4	16.9	19.3	50.0	7.8	11.3
	T8	115.2	91.9	157.3	179.2	9.2	13.7	13.1	11.9	8.3	17.5	18.7	51.8	7.7	11.7
	T9	121.0	95.0	167.7	176.8	9.3	13.8	12.4	12.2	8.4	17.8	19.3	52.1	7.0	11.6
	T10	124.1	97.3	183.5	167.3	9.9	13.7	13.0	12.5	8.3	17.6	19.3	50.1	6.3	10.9
	L1	126.1	92.1	188.4	168.2	10.0	13.8	12.9	13.0	8.4	17.3	19.3	48.2	6.2	11.0
	L2	122.6	91.9	183.2	168.3	9.5	13.9	12.4	13.1	8.6	17.9	19.4	46.1	5.8	11.0
	L3	126.4	83.4	181.0	176.9	10.1	14.1	12.7	13.4	8.7	18.2	20.4	43.7	5.3	11.7
	L4	133.2	82.7	188.5	173.3	9.2	13.6	12.4	13.6	8.4	18.8	19.3	41.6	4.4	11.8
	L5	124.8	82.6	180.8	177.3	9.2	12.9	11.8	13.8	8.0	18.5	18.3	38.0	3.4	12.2
	S1	118.8	83.3	216.1	191.2	9.4	13.7	12.7	14.8	7.9	17.3	18.8	53.1	12.3	10.0

Table S2 continued

		PZA	NSA	TPAD	TPAC	NSL	CL	NSH	CW	CH	PZW	IZD	TPW	TPLT	LW
Specimen 7	T1	93.3	117.3	157.4	196.1	8.6	16.5	29.5	22.3	11.0	21.1	22.2	44.7	5.4	13.6
	T2	113.8	105.8	146.4	198.8	9.9	16.4	25.4	22.2	10.9	23.2	23.5	47.6	6.5	15.2
	T3	115.0	105.7	138.9	209.1	10.6	17.8	23.9	16.4	11.6	25.4	23.6	54.8	10.2	16.2
	T4	116.4	106.3	153.0	202.4	11.1	17.3	22.6	16.1	11.5	26.4	24.1	61.6	10.1	16.3
	T5	117.4	103.1	159.2	198.3	11.2	17.6	21.4	16.1	10.6	26.1	23.4	65.4	9.3	16.4
	T6	121.7	98.6	164.6	188.9	11.3	18.2	19.8	15.7	10.8	26.0	24.5	71.0	10.7	16.4
	T7	118.0	97.6	170.8	184.9	12.1	18.1	19.7	15.4	11.0	25.7	24.1	70.8	10.2	16.2
	T8	117.0	96.3	175.7	179.3	11.9	18.4	18.9	15.7	11.2	25.6	24.7	72.5	9.9	16.4
	T9	119.1	90.6	183.1	170.1	11.9	18.2	18.7	16.1	11.0	26.0	24.3	74.4	8.8	16.5
	T10	128.4	87.8	189.8	164.0	12.1	18.5	18.4	16.6	11.0	27.1	25.5	72.2	9.8	16.5
	L1	135.5	87.7	200.2	165.9	13.0	19.1	18.4	16.7	11.2	27.8	26.4	68.2	9.0	16.4
	L2	129.1	84.4	195.7	166.0	13.2	19.2	18.5	17.1	11.5	27.7	26.4	66.4	9.1	16.5
	L3	133.4	84.3	196.7	169.3	12.9	18.3	19.1	17.4	11.4	28.6	26.9	61.7	8.4	16.8
	L4	127.4	83.5	191.0	177.0	12.7	18.4	18.8	17.9	11.3	28.5	26.5	61.1	7.0	16.0
	L5	118.2	85.6	194.2	184.8	12.2	17.6	19.5	18.3	11.5	27.8	24.0	55.7	5.6	15.8
	S1	113.2	85.5	213.1	206.0	12.3	18.1	19.5	19.9	10.7	26.7	24.4	77.0	14.6	13.5
Specimen 8	T1	97.3	111.8	155.0	200.0	9.1	18.2	29.6	24.1	12.6	24.9	25.7	50.1	6.5	15.7
	T2	104.4	107.3	134.8	204.1	10.0	19.0	28.9	25.2	12.7	26.8	27.1	54.3	7.5	16.4
	T3	100.2	112.5	146.8	199.8	11.1	19.4	26.3	18.4	13.4	28.1	25.8	63.9	10.9	17.6
	T4	101.1	107.5	153.9	195.9	12.3	19.2	24.7	17.7	12.6	29.3	25.6	69.0	10.1	17.5
	T5	110.7	103.7	161.3	195.6	12.3	19.1	23.2	17.7	12.1	29.4	26.5	72.3	11.3	18.4
	T6	115.5	103.9	163.1	186.8	12.5	19.6	22.6	17.2	12.2	29.8	26.1	75.3	10.9	18.2
	T7	115.8	100.0	170.8	181.6	13.1	19.9	20.8	17.2	12.2	29.5	26.3	77.3	11.2	18.7
	T8	120.4	100.6	174.1	174.7	13.4	20.1	21.2	17.2	12.4	30.4	27.3	78.5	10.8	18.8
	T9	129.6	95.3	180.0	167.8	13.1	20.0	19.0	17.4	12.3	30.9	27.1	79.0	10.3	18.2
	T10	124.5	93.9	184.7	164.5	14.4	20.3	18.7	18.3	12.2	30.2	27.8	78.5	9.8	17.5
	L1	127.3	91.7	195.1	166.0	13.4	21.0	20.5	17.9	12.4	30.5	28.2	73.7	10.0	17.2
	L2	133.4	90.0	187.7	164.1	14.4	21.0	20.8	18.1	12.4	31.1	28.9	71.1	9.1	17.7
	L3	126.0	86.9	181.7	170.5	14.0	20.7	20.5	18.4	12.8	31.8	28.4	65.9	7.7	18.0
	L4	127.9	88.3	181.5	176.2	13.2	20.1	20.7	18.9	12.8	32.2	29.2	63.3	6.5	17.3
	L5	117.5	87.1	192.6	174.4	13.2	19.6	20.8	19.8	12.7	32.0	28.2	58.2	6.2	18.0
	S1	115.9	86.8	216.4	205.0	14.1	20.3	20.4	20.8	12.5	31.1	27.2	81.7	15.2	15.7

All angular measurements (PZA, NSA, TPAD, TPAC) in degrees, all linear measurements in millimetres. See text for abbreviations.

Table S7. Post-hoc tests of between-subject variance in stiffness by direction and joint

Pairwise comparisons		Mean Difference	S.E.	*P*	95% Confidence Interval	
Dorsal extension	Lateral flexion	0.1053*	0.0380	0.0181	0.0137	0.1969
	Ventral flexion	-0.0070	0.0383	1.0000	-0.0994	0.0854
Lateral flexion	Dorsal extension	-0.1053*	0.0380	0.0181	-0.1969	-0.0137
	Ventral flexion	-0.1123*	0.0380	0.0103	-0.2039	-0.0207
Ventral flexion	Dorsal extension	0.0070	0.0383	1.0000	-0.0854	0.0994
	Lateral flexion	.1123*	0.0380	0.0103	0.0207	0.2039
T1-2	T3-4	-0.1674	0.0644	0.2783	-0.3709	0.0361
	T5-6	-0.1880	0.0635	0.0942	-0.3885	0.0125
	T7-8	-0.1581	0.0635	0.3768	-0.3586	0.0425
	T9-10	-0.2348*	0.0631	0.0068	-0.4339	-0.0356
	L1-2	-0.2743*	0.0631	0.0006	-0.4734	-0.0751
	L3-4	-0.3942*	0.0626	0.0000	-0.5921	-0.1964
	L5-S1	-0.8440*	0.0639	0.0000	-1.0460	-0.6420
T3-4	T1-2	0.1674	0.0644	0.2783	-0.0361	0.3709
	T5-6	-0.0206	0.0630	1.0000	-0.2195	0.1783
	T7-8	0.0093	0.0630	1.0000	-0.1895	0.2082
	T9-10	-0.0674	0.0625	1.0000	-0.2649	0.1301
	L1-2	-0.1069	0.0625	1.0000	-0.3044	0.0906
	L3-4	-0.2268*	0.0621	0.0089	-0.4230	-0.0306
	L5-S1	-0.6766*	0.0634	0.0000	-0.8769	-0.4763
T5-6	T1-2	0.1880	0.0635	0.0942	-0.0125	0.3885
	T3-4	0.0206	0.0630	1.0000	-0.1783	0.2195
	T7-8	0.0299	0.0620	1.0000	-0.1659	0.2258
	T9-10	-0.0468	0.0616	1.0000	-0.2412	0.1477
	L1-2	-0.0863	0.0616	1.0000	-0.2807	0.1082
	L3-4	-0.2062*	0.0611	0.0242	-0.3993	-0.0131
	L5-S1	-0.6560*	0.0625	0.0000	-0.8533	-0.4587
T7-8	T1-2	0.1581	0.0635	0.3768	-0.0425	0.3586
	T3-4	-0.0093	0.0630	1.0000	-0.2082	0.1895
	T5-6	-0.0299	0.0620	1.0000	-0.2258	0.1659
	T9-10	-0.0767	0.0616	1.0000	-0.2712	0.1177
	L1-2	-0.1162	0.0616	1.0000	-0.3106	0.0782
	L3-4	-0.2361*	0.0611	0.0040	-0.4292	-0.0430
	L5-S1	-0.6860*	0.0625	0.0000	-0.8833	-0.4886
T9-10	T1-2	0.2348*	0.0631	0.0068	0.0356	0.4339

	T3-4	0.0674	0.0625	1.0000	-0.1301	0.2649
	T5-6	0.0468	0.0616	1.0000	-0.1477	0.2412
	T7-8	0.0767	0.0616	1.0000	-0.1177	0.2712
	L1-2	-0.0395	0.0611	1.0000	-0.2325	0.1535
	L3-4	-0.1594	0.0607	0.2564	-0.3511	0.0322
	L5-S1	-0.6092*	0.0620	0.0000	-0.8052	-0.4133
L1-2	T1-2	0.2743*	0.0631	0.0006	0.0751	0.4734
	T3-4	0.1069	0.0625	1.0000	-0.0906	0.3044
	T5-6	0.0863	0.0616	1.0000	-0.1082	0.2807
	T7-8	0.1162	0.0616	1.0000	-0.0782	0.3106
	T9-10	0.0395	0.0611	1.0000	-0.1535	0.2325
	L3-4	-0.1199	0.0607	1.0000	-0.3116	0.0717
	L5-S1	-0.5698*	0.0620	0.0000	-0.7657	-0.3738
L3-4	T1-2	0.3942*	0.0626	0.0000	0.1964	0.5921
	T3-4	0.2268*	0.0621	0.0089	0.0306	0.4230
	T5-6	0.2062*	0.0611	0.0242	0.0131	0.3993
	T7-8	0.2361*	0.0611	0.0040	0.0430	0.4292
	T9-10	0.1594	0.0607	0.2564	-0.0322	0.3511
	L1-2	0.1199	0.0607	1.0000	-0.0717	0.3116
	L5-S1	-0.4498*	0.0616	0.0000	-0.6444	-0.2552
L5-S1	T1-2	0.8440*	0.0639	0.0000	0.6420	1.0460
	T3-4	0.6766*	0.0634	0.0000	0.4763	0.8769
	T5-6	0.6560*	0.0625	0.0000	0.4587	0.8533
	T7-8	0.6860*	0.0625	0.0000	0.4886	0.8833
	T9-10	0.6092*	0.0620	0.0000	0.4133	0.8052
	L1-2	0.5698*	0.0620	0.0000	0.3738	0.7657
	L3-4	0.4498*	0.0616	0.0000	0.2552	0.6444

P-values reflect Bonferroni correction for multiple comparisons.
The error term is Mean Square (Error) = 0.065.